AD NUMBER

AD815676

LIMITATION CHANGES

TO:

Approved for public release; distribution is unlimited. Document partially illegible.

FROM:

Distribution authorized to U.S. Gov't. agencies and their contractors; Critical Technology; FEB 1967. Other requests shall be referred to Air Force Technical Application Center, VELA Seismological Center, Washington, DC 20333. Document partially illegible. This document contains export-controlled technical data.

AUTHORITY

usaf ltr, 25 jan 1972

TR66-90

TECHNICAL REPORT NO. 66-90

EXPERIMENTAL INVESTIGATION OF THERMAL NOISE

GEOTECH
A TELEDYNE COMPANY

TECHNICAL REPORT NO. 66-90

EXPERIMENTAL INVESTIGATION OF THERMAL NOISE

by

Wayne Trott

Sponsored by

Advanced Research Projects Agency
Nuclear Test Detection Office
ARPA Order No. 624

Availability

Qualified users may request copies of
this document from:
Defense Documentation Center
Cameron Station
Alexandria, Virginia 22341

Acknowledgement

This research was supported by the Advanced Research Projects Agency, Nuclear Test Detection Office, under the VELA-UNIFORM Program and was accomplished under the technical direction of the Air Force Technical Applications Center under Contract No. AF 33(657)-16406.

GEOTECH
A TELEDYNE COMPANY
3401 Shiloh Road
Garland, Texas

20 February 1967

IDENTIFICATION

AFTAC Project No:	VELA T/6706
Project Title:	Long-Period Seismograph Development
ARPA Order No:	624
ARPA Program Code No:	6F10
Name of Contractor:	Teledyne Industries, Geotech Division Garland, Texas
Contract No:	AF 33(657)-16406
Effective Date of Contract:	15 June 1966
Amount of Contract:	$172,800
Project Manager:	Richard M. Shappee BR 8-8102, Area Code 214

CONTENTS

ILLUSTRATIONS

ILLUSTRATIONS, (Continued)

ABSTRACT

The primary objective of the experimental investigation of thermal noise was to verify and apply an analysis derived by National Bureau of Standards which can spectrally describe thermal energy in seismographs. When applied to a typical, operational, long-period seismograph, the NBS analysis shows the need for 10 kg inertial mass for a system magnification of about 130 k at 25 sec. Two experiments were designed to verify the NBS analysis. The first experiment was conducted to determine and verify the thermal energy spectrum for a seismometer or galvanometer connected to a resistive load. As a result of excessive uncancelled seismic inputs, the first experiment was only partially successful. The second experiment was conducted to determine and verify the thermal energy spectrum of the galvanometer in a seismometer-galvanometer combination. The results of the second experiment were agreement with theory. There was sufficient agreement between the empirical and theoretical spectra to verify the validity of the NBS analysis. The NBS analysis was therefore recommended for present use, but repetition of the first experiment in a seismically quieter location was recommended to further verify the analysis.

EXPERIMENTAL INVESTIGATION OF THERMAL NOISE

1. INTRODUCTION

1.1 AUTHORITY

The work described in this report was performed by Geotech, A Teledyne Company, in fulfillment of the requirements set forth in Task 1a of the Statement of Work of Project VT/6706, Contract AF 33(657)-16406. A copy of the Statement of Work is included with this report as appendix 1.

1.2 PURPOSE

The purpose of the investigation was twofold. First, it was intended to briefly review earlier work done related to the general subject of thermal noise and the effects of such noise on measurement processes. It was further intended to more thoroughly investigate and apply some of the later thermal noise work that was directed specifically at a major seismic instrumentation problem. This problem is the determination of minimum inertial mass required for a seismometer when a given system magnification is necessary. Second, it was intended to conduct exacting experiments to verify some of the results of the later work so that these results can be more confidently used in instrument and system design.

1.3 PREVIOUS WORK

The basic design features of the torsional pendulums used in the experimental effort on this study, such as the vacuum-tight housing, housing support system, suspension support system, and mirror locking details evolved directly from the work of Task 1b, Galvanometers, Project VT/072. Detail design and fabrication of most of the parts for the pendulums and conceptual design of the experimental work were completed on Task 1j, Experimental Investigation of Thermal Noise, Project VT/072. These efforts are described in Geotech Technical Report (TR) No. 64-133, Galvanometers, Project VT/072 and TR No. 64-127, Interim Report on the Experimental Investigation of Thermal Noise, Project VT/072.

1.4 SCOPE

Concise summaries of classically accepted early papers on thermal noise are contained in section 2.1 of this report. These summaries are qualitative in nature. Brief discussions of later efforts, some of those specifically directed at seismic problems, are contained in section 2.2. This later work consisted largely of work done at the RCA Laboratories, Radio Corporation of America (RCA) and work done at the National Bureau of Standards (NBS). The RCA work was accomplished under AFOSR Contract Numbers AF 49(638)-1080 and AF 49(638)-1456. The NBS work was theoretical and is contained in unpublished private correspondences between Geotech and NBS personnel. Other papers on the subject of thermal noise are listed in section 7 of this report.

The work done at NBS resulted in equations which spectrally characterize thermal noise in terms of a common set of seismograph control parameters. These equations were considered the key equations of this study, and as such, the major efforts of the study were devoted to the application of these equations and their experimental verification. FORTRAN computer programs were written, based upon the NBS equations, and the thermal noise in hypothetical systems was spectrally characterized.

Section 3 contains a description of the experimental apparatus and procedures used to acquire the empirical data.

Section 4 contains descriptions of the experimental data. The data analysis technique is briefly described and theoretical and empirical spectra are graphically compared for the hypothetical systems.

Conclusions and recommendations are contained in sections 5 and 6, respectively.

Appendix 2 contains the complete development of the NBS equations.

1.5 ACKNOWLEDGEMENT

While the references listed in section 7 of this report contain all sources of information used, special acknowledgement is given to Dr. Dan Johnson, Mr. Harry Matheson, and Mr. Walter J. Gilbert of NBS. Mr. Matheson and Mr. Gilbert were responsible for the NBS equations discussed in section 2 of this report and the development of these equations contained in appendix 2. Dr. Johnson rendered valuable assistance in the basic optical layout discussed in section 3.

2. THEORY

2.1 THERMAL NOISE

2.1.1 Brownian Motion

Thermal agitation of particles has been observed for over 100 years. Barnes and Silverman, in a 1934 paper in the Reviews of Modern Physics, briefly summarized the evolutionary thinking on the subject to that date. According to Barnes and Silverman, naturalist Robert Brown observed a random motion of pollens he was studying in a suspension in 1827. It was first thought that these pollens and other similarly observed particles were alive. Tests with very old particles, some even from the Egyptian Sphinx, proved that the motion was not due to the action of live particles. Various other explanations for the random motions were subsequently disproved. The first published information which correctly identified the phenomenon was a paper written by Delsaulx in 1877. In that paper, Delsaulx showed that the motion of a particle in a fluid was caused by random energy received from constituents of the fluid. Several other papers have been written since which verify the idea advanced by Delsaulx. Noteable are papers by Gouy in 1888, Einstein in 1906, V. Smoluchowski in 1906, and Perrin in 1909. It was thus established, and is now accepted, that a particle or body in fluid medium will experience a random motion caused by energy imparted to the body by constituents of the fluid. The imparted energy from the constituents of the fluid is directly related to the absolute temperature of the fluid as well as to other factors. The random motion of particles or bodies in a fluid resulting from thermal agitation is commonly called Brownian motion. In considering a seismometer mass as a body and the air molecules of the atmosphere as constituents of a fluid, it can be assumed that a seismometer mass will experience a random motion because of thermal agitation of the air molecules. The same assumption can be logically made for a galvanometer armature.

2.1.2 Johnson Noise

In a paper published in the Physical Review in July of 1928, Dr. J. B. Johnson made the observation and measurement of a thermal electromotive force in electrical conductors. From empirically derived data, Johnson concluded that any electrical conductor has between its terminals a thermally originating EMF, the mean-square value of which is proportional to the electrical resistance and absolute temperature of the conductor.

Also in the July 1928 issue of the Physical Review is a well-known paper by Nyquist in which he theoretically verified the results of Johnson's tests. Nyquist's conclusions were essentially the same as those of Johnson in that the mean-square voltage at the terminals of a conductor resulting from thermal agitation is a function only of frequency bandwidth, resistance, and

temperature. It was established and is now accepted that electrical conductors contain an equivalent random-noise generator caused by thermal agitation of the electrical current carriers. This phenomenon is commonly called Johnson noise. In considering a seismometer or galvanometer coil, it can be assumed that a random voltage resulting from thermal agitation will appear across the terminals of the galvanometer and a motion of the galvanometer armature can result.

2.1.3 Spectral Features and RMS Values of Thermal Noise

As stated, thermal noise in a seismometer and a galvanometer come from several different sources. It can result from the irregular bombardment of air molecules on the mass and from the random movement of electrons in the electrical circuit. Any loose elements, such as resistors or dashpots, which are coupled to the spring-mass system of the seismometer will act as noise sources. The coupling of any other system to a spring-mass system will not alter the long-term average of the kinetic or potential energy of the spring-mass system if the temperatures of the two systems are equal. Any change in the long-term average energy of the spring-mass system would mean that energy was exchanged by two systems initially at the same temperature. Such an exchange would violate the second law of thermodynamics.

While the long-term or rms value of the noise energy of a spring-mass combination is independent of its coupling to other systems which are at the same temperature, the special distribution of the noise energy is not necessarily independent of the coupling.

Consider a seismometer or galvanometer which is damped at some value by a combination of air and electrical damping. If the air damping is removed and the electrical damping increased so that the total damping remains the same, the rms value of the noise energy will not be altered. However, it is possible that the spectral distribution of the noise energy may be different. As another example, consider two identical moving-coil seismometers at the same temperature and damped at the same value. Let one be coupled to a resistive load, and the other to a galvanometer. Again, the rms value of the thermal noise of the two seismometers will be the same, but the spectral distribution of this noise energy may not be the same.

While it is true that much theoretical and experimental work has been done on thermal noise, most of this work has been to confirm that its value is $1/2\ kT$ for each coordinate required to describe the position and momentum of a system, where k is Botzmann's constant and T is the absolute temperature. This fact is true for any system, and as previously stated, is independent of coupling. Since the spectral distribution is a function of coupling, it can only be investigated for a specific case.

2.2 SEISMOGRAPH ANALYSIS

The studies conducted at RCA were broad in scope. Briefly, one of the results of the work at RCA indicated that refrigeration of a damping resistor external to a seismometer would be impractical as a means to reduce thermal noise effects in a seismograph. Further, the RCA work resulted in the conclusion that the thermal noise characteristics of a seismometer improves as internal damping losses are minimized. The RCA studies also revealed an apparent improvement in noise characteristics of a seismometer-amplifier combination by the use of certain feedback techniques.

The RCA studies were conducted during the period from 15 June 1961 to 14 January 1966 and are reported in detail in several reports which are listed in the reference section of this report.

2.2.1 NBS Analysis

A seismograph will, as pointed out above, contain a thermally induced output resulting from both Brownian motion and Johnson noise. Nyquist in his 1928 paper briefly discussed the relationship and indicated the equivalence of Brownian motion to Johnson noise. More recently, a mathematical model of a seismograph with its thermal agitation noise generators has been described (Matheson and Gilbert, 1964). The Matheson and Gilbert analysis directly relates Brownian motion in seismograph components to Johnson noise. In equations describing the equivalent circuit of the seismometer-galvanometer combination, the internal damping terms of the seismometer and galvanometer were replaced by their equivalent virtual resistors. The noise analysis was then treated as if the noise generators were of the Johnson-noise variety. The complete NBS development is given in appendix 2.

The NBS analysis considered two seismometer-load combinations, a seismometer or galvanometer connected to a resistive load and a seismometer-galvanometer combination. The defining equations from appendix 2 for the resistive load case can be written as:

$$|\theta|^2 = \frac{4\,(\lambda_g + \lambda_\theta)\,\omega/\omega_g\,kT}{\pi U\,(1 - \omega^2/\omega_g{}^2)^2 + 4\,(\lambda_\theta + \lambda_g)^2\,\omega^2/\omega_g{}^2} \qquad (1)$$

where $|\theta|^2$ is the spectral density in $(\text{radians})^2$/octave of the thermally induced angular position. All other parameters are defined in the glossary of terms at the end of this report. The analogus circuit for the resistive load case is shown in figure 1.

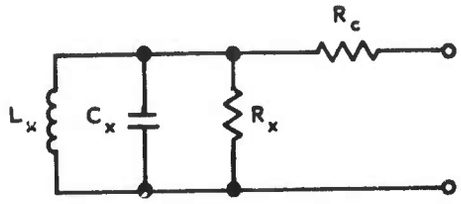

Figure 1. Analogus circuit for seismometer (or galvanometer), excluding generators

Similarly, the spectral density of angular position of the galvanometer armature in the combination case, can be written as:

$$|\theta|^2 = \frac{4\Lambda_g}{U(D_r^2 + D_i^2)} \left[4\Lambda_o^2 (1-\alpha^2)x^2 + \frac{\omega_g^2}{\omega_o^2}\left(\frac{\omega_o^2}{\omega_g^2} - x^2\right)\right] \frac{kT}{T} \quad (2)$$

where:

$$D_r = (1-x^2)\left(\frac{\omega_o^2}{\omega_g^2} - x^2\right)\frac{\omega_g}{\omega_o} - 4x^2(\Lambda_o\Lambda_g - \lambda_o\lambda_g)$$

$$D_i = 2\Lambda_g x \left(\frac{\omega_o^2}{\omega_g^2} - x^2\right)\frac{\omega_g}{\omega_o} + 2\Lambda_o x(1-x^2)$$

$$\alpha = \lambda_g\lambda_o/\Lambda_g\Lambda_o$$

$$x = \omega/\omega_g$$

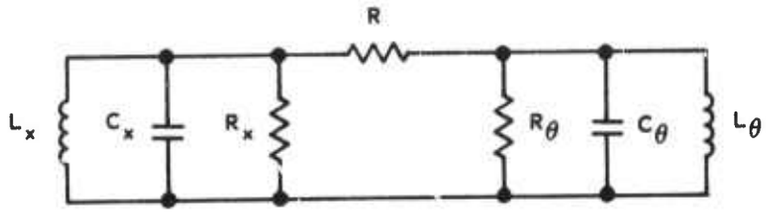

Figure 2. Analogus circuit for seismometer-galvanometer combination, excluding generator

By comparing the earth motion-to-galvanometer rotation transfer characteristics for a given seismograph to equations 1 and 2 above, the earth-motion equivalent to thermal-noise level can be established. This motion equivalent to noise level thus defines a spectrally characterized lower limit for detection.

An expression from which the galvanometer rotation can be related to earth motion is equation 6.2.2 in NBS Report 7454. This equation can be written as:

$$2\alpha \Lambda_m \omega_m \sqrt{\frac{M}{K}} \left(\frac{y}{\theta}\right) = 2\Lambda_o \omega_o \left(\frac{\omega_g^2 - \omega^2}{\omega^2}\right) + 2\Lambda_g \omega_g \left(\frac{\omega_o^2 - \omega^2}{\omega^2}\right)$$

$$- j\omega \left[\left(\frac{\omega_g^2 - \omega^2}{\omega^2}\right) \left(\frac{\omega_o^2 - \omega^2}{\omega^2}\right) + 4(\alpha^2 - 1) \Lambda_m^2 \frac{\omega_m^2}{\omega^2}\right] \qquad (3)$$

The analysis technique outlined above is valid only for instruments for which electrical inductance is negligible.

2.2.2 Application of NBS Analysis to Operational System

The analysis technique outlined in section 2.2.1 was applied to the advanced long-period system in a typical field configuration. The advanced long-period system is described in detail in Geotech Technical Report (TR) No. 63-25, Advanced Long-Period System. Figure 3 shows the seismometer-galvanometer combination of the advanced long-period system reduced to a form suitable for analysis.

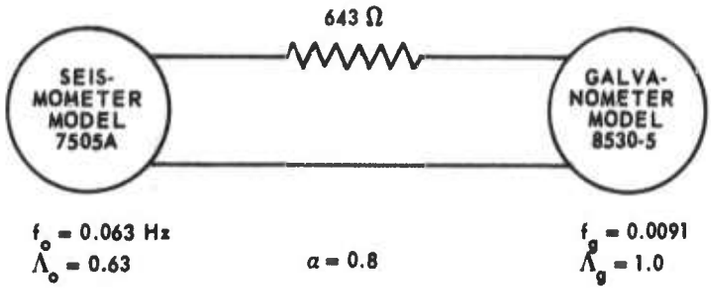

A. SEISMOMETER-GALVANOMETER COMBINATION

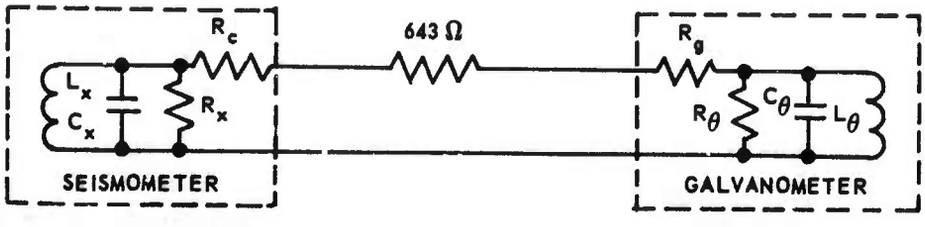

R_c = COIL RESISTANCE
R_x ≡ INTERNAL LOSSES
L_x ≡ SPRING
C_x ≡ MASS

R_g = COIL RESISTANCE
R_θ ≡ INTERNAL LOSSES
L_θ ≡ SPRING
C_θ ≡ ARMATURE INERTIA

B. ELECTRICAL ANALOG OF ADVANCED LONG-PERIOD SYSTEM, EXCLUDING GENERATORS

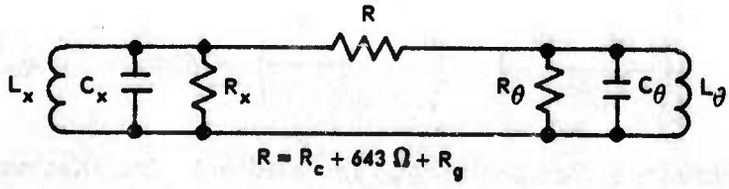

C. ELECTRICAL ANALOG OF ADVANCED LONG-PERIOD SYSTEM REDUCED TO A BASIC FORM, EXCLUDING GENEPATORS

Figure 3. Seismometer-galvanometer combination in advanced long-period system

G 2360

In addition to the seismometer-galvanometer combination, the advanced long-period system includes a Model 5240A phototube amplifier (PTA) and a high-gain channel passband filter, Model 6824-15. Figure 4 shows the frequency response of the system and is included for reference. For purposes of the analyses, it was assumed that 1 mm p-p was the maximum allowable record displacement resulting from the thermal noise and that only the high-gain channel of the system was of interest. It was further assumed that 6 X rms values were equivalent to long-term p-p values. Narrow-band and broad-band analyses of the system are described below.

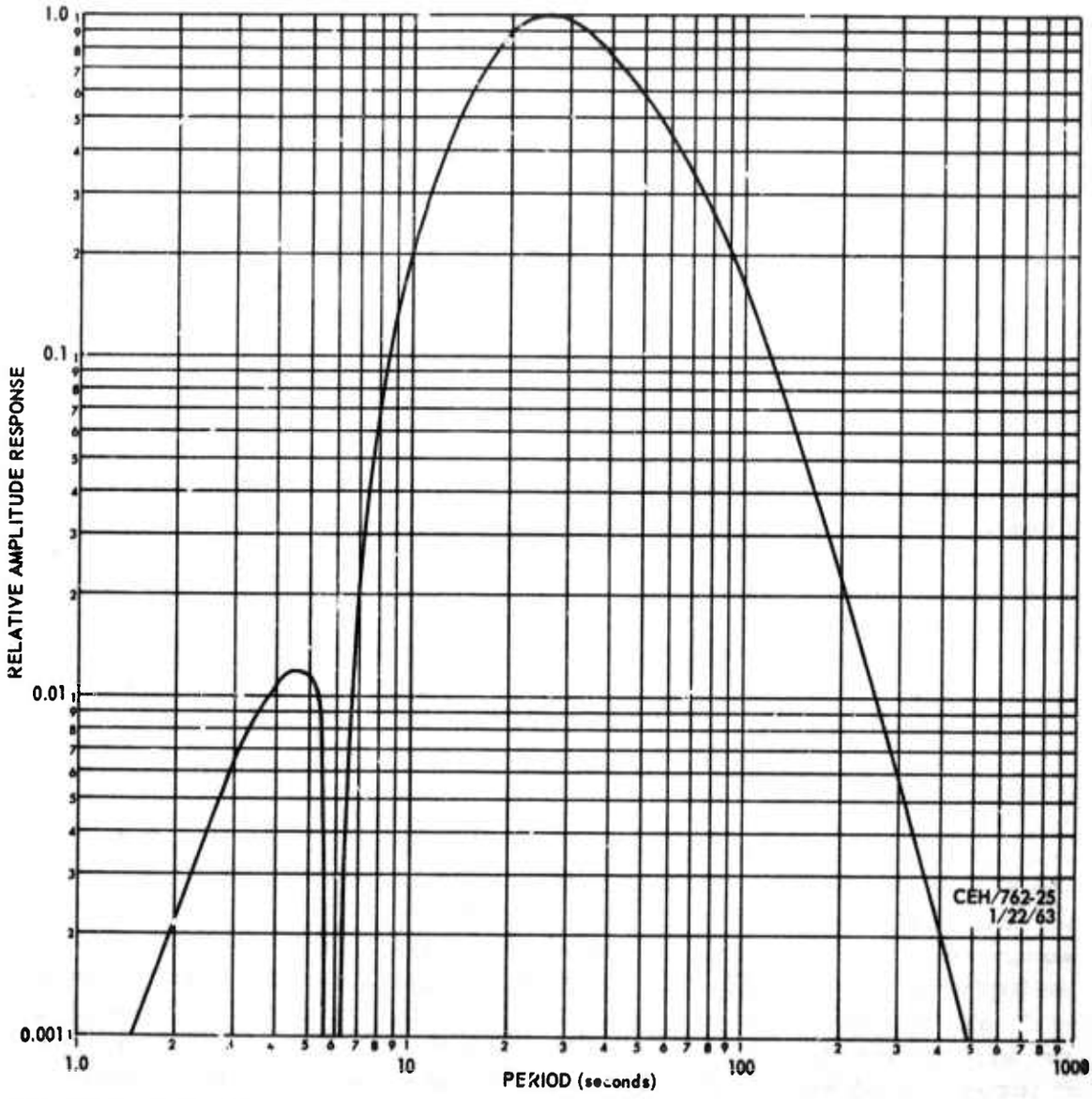

Figure 4. Relative amplitude frequency response of the advanced long-period system

G 2695

When considering narrow pass bands, data points from equation (2) can be divided by squared values of data points from equation (3) which is expressed as $y/\theta = f(\Lambda_o, \Lambda_g, \omega_o, \omega_g, M, K, \alpha)$, yielding a spectral relationship between thermal noise and detectable earth motion. This relationship is shown in figure 5 for the advanced long-period system as are similar relationships for two hypothetical systems, one with a 1 kg mass seismometer and one with a 100 kg mass seismometer. In examining figure 5, it is apparent that the system is most severely limited by thermal noise at the longer periods. To illustrate the use of figure 5 for a narrow pass band at the longer periods, consider a system with 10 kg mass seismometer from which data in a 1/4 octave bandwidth centered on 100 sec is of interest. (It should be noted that a 1/4 octave wide pass band is possibly undesirable and probably impractical.) From figure 5, the spectral density at 100 sec is 13 $m\mu^2$/octave. For the 1/4-octave pass band, the equivalent mean-square thermal noise is 1/4 octave x 13 $m\mu^2$/octave or 3.25 $m\mu^2$. The long-term peak-to-peak value of the thermal noise is equivalent to approximately 6 x $\sqrt{3.25\ m\mu^2}$ or 11 mμ. By dividing 1 mm p-p by 11 mμ p-p, a maximum magnification of about 90K at 100 sec is predicted. (If thermal noise were the only limitation, a magnification of about 2500 K would be possible for a 1/4 octave wide pass band centered on 25 sec.) Similarly, a maximum magnification of about 30 K could exist in the 1/4-octave pass band centered on 100 sec for the 1 kg case represented in figure 5; and for the 100 kg case, a magnification at 100 sec of about 300 K would be possible.

An analysis considering the complete pass band was conducted as follows. The initial step was to spectrally characterize the root-mean-square thermal noise in the galvanometer armature by taking the square root of mean-square values obtained from equation (2). Each point on the resulting spectrum was then multiplied by the absolute amplitude response of the high-gain channel filter. The resulting spectrum was then multiplied by the PTA sensitivity, 700 volts/radian, yielding the rms spectrum of the thermal noise as it would appear at the PTA output. By squaring each point on this spectrum and integrating the results, the mean-square value of the thermal noise was obtained: 9.1 (10)-8 volts^2. By taking the square root of this value and then multiplying by 6, an estimate of the PTA long-term, peak-to-peak output resulting from thermal noise was obtained: 1.81 mV p-p. The earth motion at 25 sec which also results in a PTA output of 1.81 mV p-p is 7.7 mμ p-p. Thus, 7.7 mμ p-p earth motion at 25 sec can be considered equivalent to the thermal noise in the complete pass band of the high-gain channel of the advanced long-period system. This equivalence can be demonstrated by multiplying 7.7 mμ p-p by the seismometer-galvanometer combination gain at 25 sec obtained from equation (3): 701 radians/meter. The resulting product is then multiplied by the PTA sensitivity, 700 volts/radian, and the filter gain at 25 sec: 0.48. The result of these multiplications, when multiplied by 10^{-9} meter/mμ, yields the 1.81 mV p-p. Dividing the 1 mm by 7.7 mμ yields a maximum magnification at 25 sec of about 130 K. Similarly, 1 kg and 100 kg seismometers would yield maximum magnifications of 40 K and 400 K, respectively.

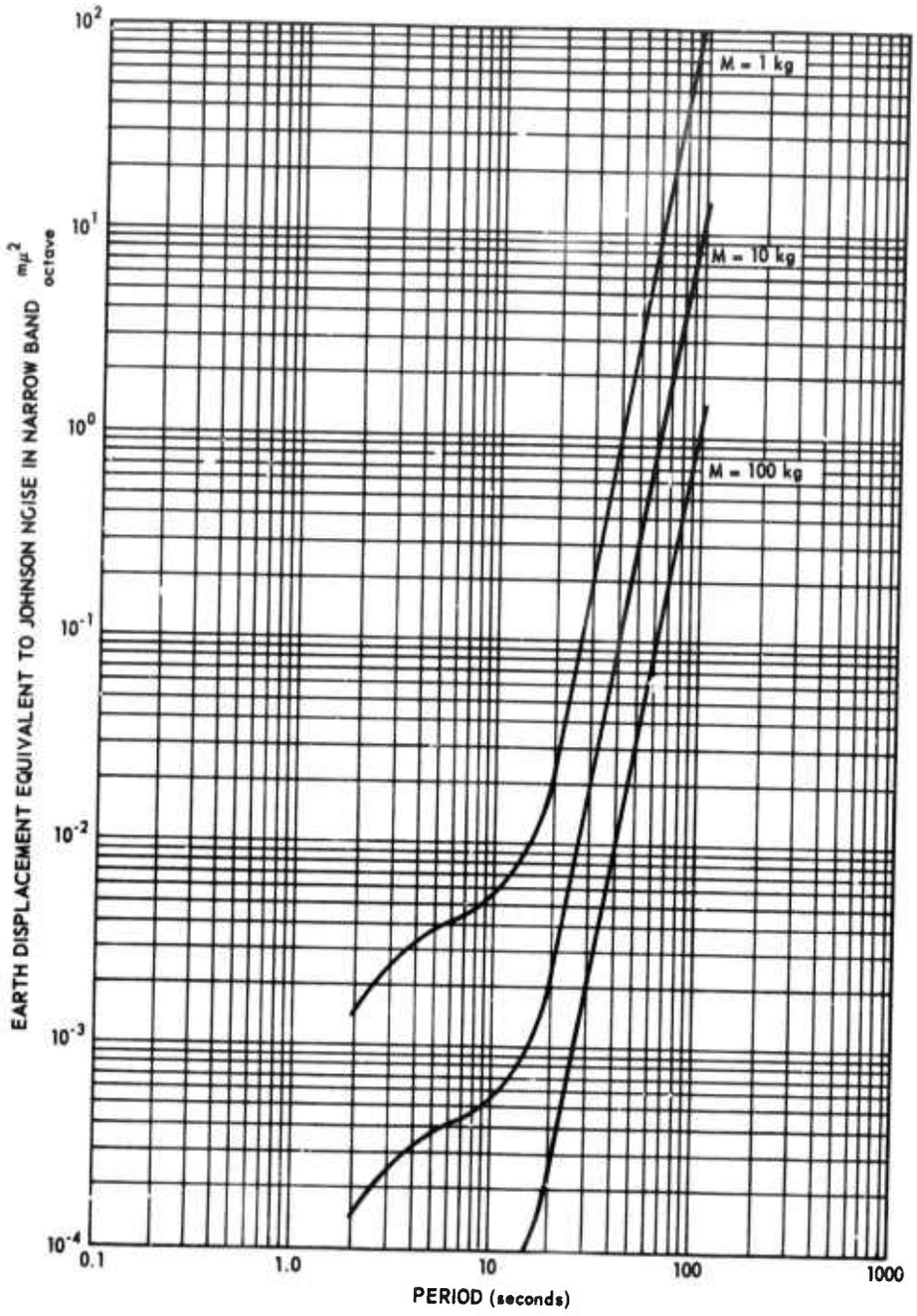

Figure 5. Earth displacement equivalent to thermal noise in advanced long-period system

G 2696

3. EXPERIMENTAL EQUIPMENT AND PROCEDURES

3.1 GENERAL

The purpose of the experimental effort was to investigate the spectral distribution of noise energy in seismometers and galvanometers and their connections in terms of a commonly used set of seismograph parameters. Subsequent comparisons of the thermal-noise spectrum with a typical seismic-noise spectrum will enable the ultimate magnification of a typical seismograph to be expressed in terms of its various parameters.

The experimental effort in this study investigation was divided into two parts called experiment 1 and experiment 2. Experiment 1 was designed to determine the spectral distribution of thermal-noise energy in a seismometer or galvanometer with a resistive load, thereby verifying equation 1 in section 2.2.1. The purpose of experiment 2 was to determine the spectral distribution of thermal-noise energy in a seismometer-galvanometer combination and as a result, verify equation 2 in section 2.2.1.

3.2 DESCRIPTION OF APPARATUS AND EQUIPMENT

The laboratory selected for the tests consisted of two rooms, one of which contained an isolated pier. The various pendulums, the thermal energy of which was to be determined, were located on the pier with other experimental apparatus and all controlling equipment such as function generators, recorders, and signal-conditioning amplifiers were located in the adjoining room so that all calibrations and adjustments could be made without entering the pier room and disturbing the sensitive instruments. The configuration for experiment 1 was that of a single torsion pendulum and for experiment 2 was that of two torsion pendulums coupled together.

Torsion pendulums were used to minimize the effects of pier motions which were predominately translational. The same experimental techniques and equipment were used for both experiment 1 and experiment 2 where possible.

3.2.1 Experiment 1

Experiment 1 was designed so that coherent outputs from two like pendulums would be subtracted, thereby minimizing inputs such as rotational components of pier motion. Instantaneous values of incoherent pendulum outputs added directly, however. Very careful attention was given to design and assembly details concerning the pendulums so that two like ones could be fabricated. A torsion pendulum is shown in figure 6 where key features are indicated. The careful matching required that much attention be given to the armatures and suspension fibers. Each armature consisted of a symmetrical quartz

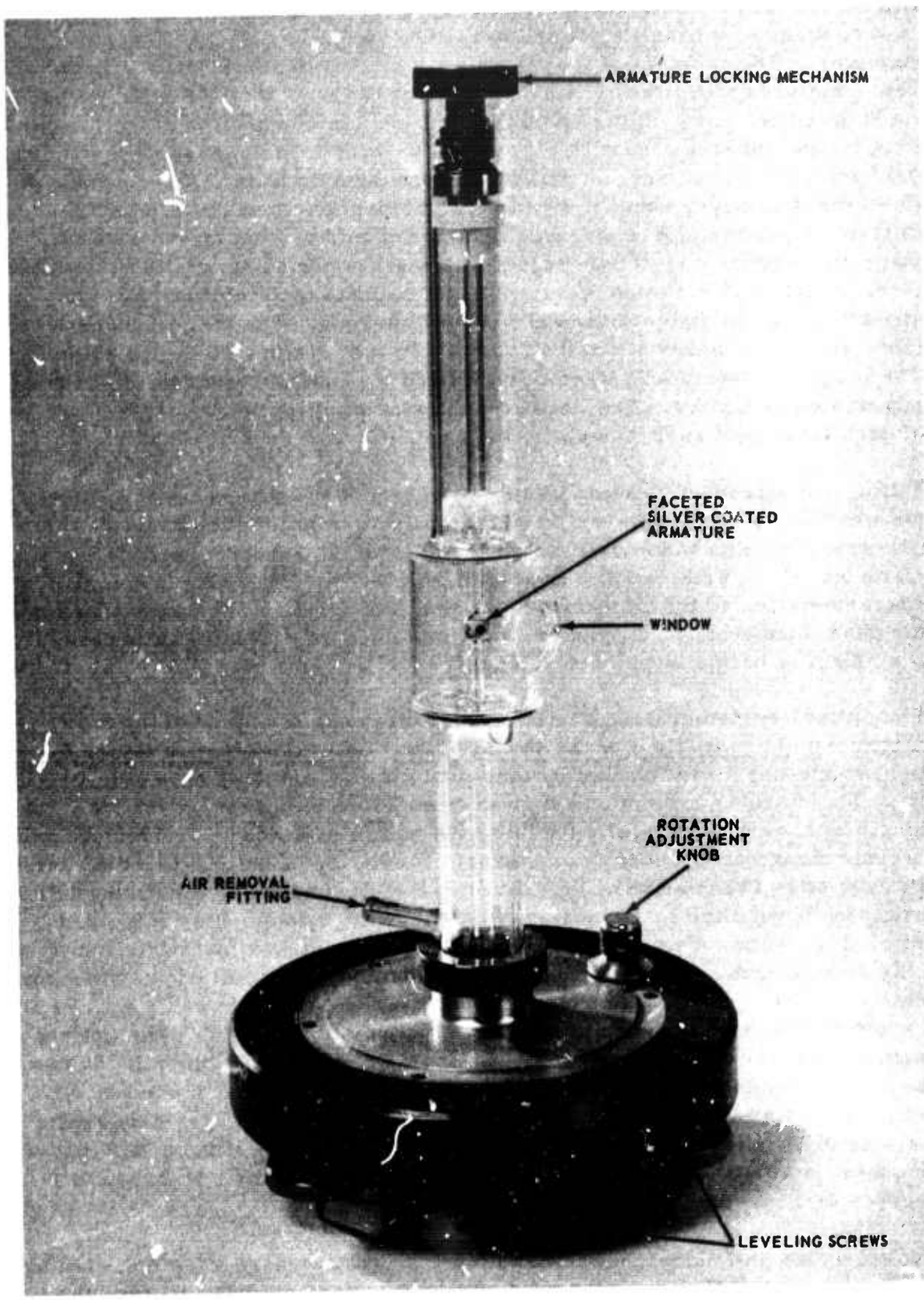

Figure 6. Torsion pendulum

G 2363

sphere 9.5 mm in diameter on which two flats were ground using special care to insure that the flats were parallel, optically flat, and identical in diameter. The moment of inertia of each sphere was $9.05\ (10)^{-9}$ kg m^2. The armatures were then coated with silver $3\ (10)^{-3}$ mm thick using the rochelle salts chemical deposition technique. In conjunction with the optical flats on the spheres, the silver coatings provided the necessary pendulum mirrors, and in conjunction with external magnetic fields, the coatings provided the necessary conductors for electromagnetic pendulum damping. Control of pendulum damping was accomplished by shunting the external magnetic structures. These structures were made using available magnets from Model 6840 seismometers. These magnets were cylindrical and were about 102 mm in diameter and about 114 mm long. The magnets were made from Alnico 5. Special mountings and pole pieces were made for the magnets. The magnetic structures were charged and the uniformity of the field in each gap was satisfactory. The field strengths in the gaps were within 3 percent of each other and each was about 1800 gauss.

Fittings to attach suspension fibers were attached to the spheres. The suspension fibers were individually selected from a collection of quartz fibers. The selection was made on the basis of matching pendulum periods and the diameter of the selected fibers was about 10^{-5} m. Thus, the critical internal characteristics of the pendulums, moments of inertia of the armatures and torsional constants of the fibers, were matched as carefully as practically possible and damping was controllable.

The optical system which provided coherent cancellations utilized some basic features and assemblies of the Model 4300 PTA. Referring to figure 7, the light source, S, was focused by lens system, LS, on the pendulum mirror, P_1. The distance from P_1 to L_1 and from L_2 to P_2 was equal to the focal length of L_1 and L_2 thereby focusing the image at P_1 on P_2. This optical arrangement was necessary to prevent translation of the image on P_2 when P_1 rotated. Translation of the image of S at P_2 caused by rotation of P_1 would have resulted in a translation at the beam splitter even if P_2 had rotated the same amount as P_1. In other words, it was not sufficient to have only angular subtraction of P_1 and P_2 rotations, but translation of the image on P_2 caused by P_1 rotation was intolerable. Focusing S on P_1 and P_2 also resulted in an efficient use of the available quantity of light. The optical-path distances from the stop O to L_1, from L_1 to L_2, and from L_2 to the beam splitter lens (BL) was such that the image of O was focused on BL. The shape of O was a square with sides about 25 mm long. Thus, coherent rotations of P_1 and P_2 caused no translation of the image of O on BL, but any incoherent rotations of P_1 and P_2 resulted in a translation at BL, and corresponding output from the phototubes resulted.

Calibrations and noise checks of the optical system were accomplished by replacing one of the torsion pendulums with a fixed mirror and the other with a calibrated galvanometer whose suspension was much stiffer than those in the pendulums.

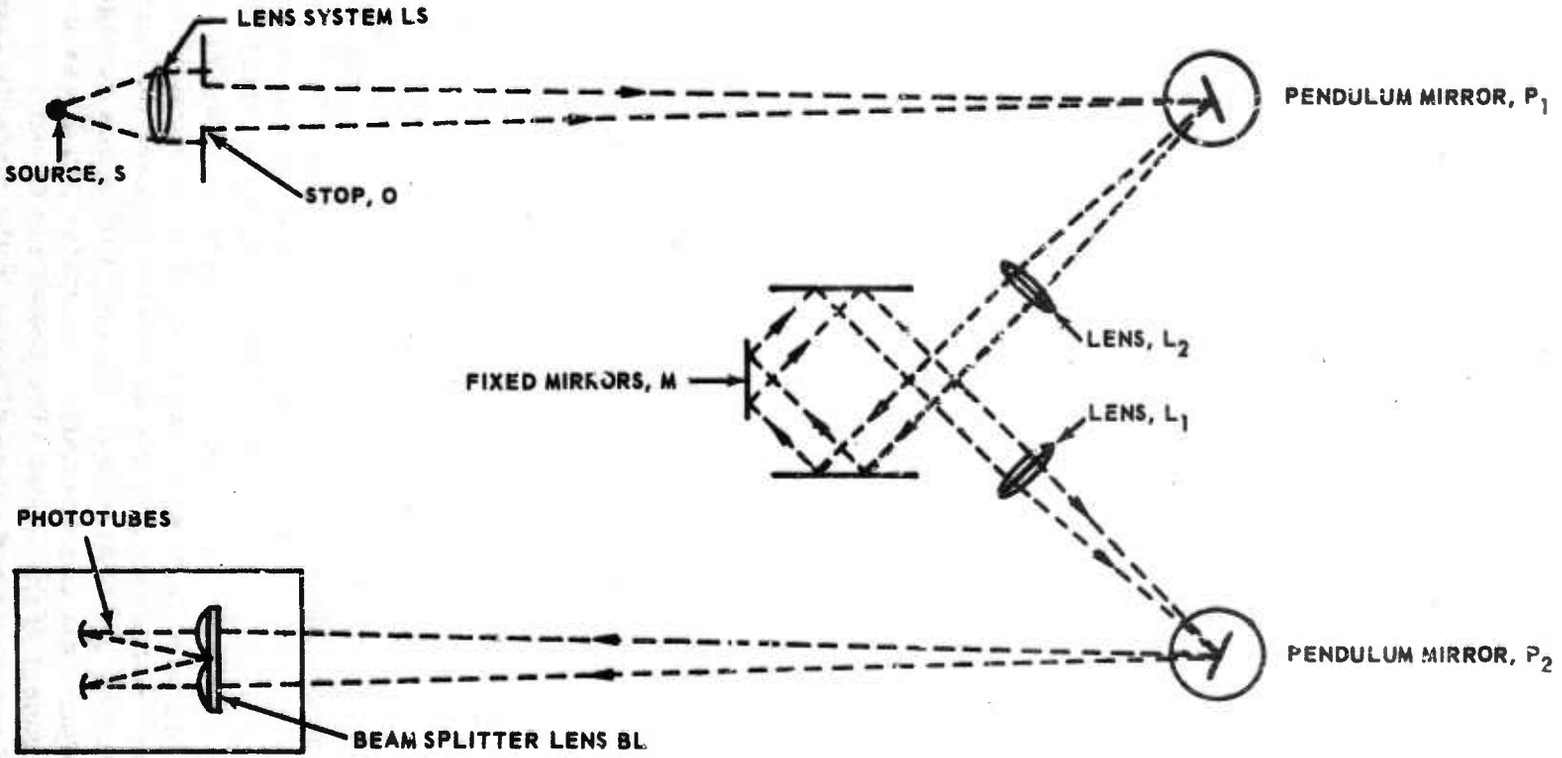

Figure 7. Ray diagram for torsion pendulum optical system

G 2364

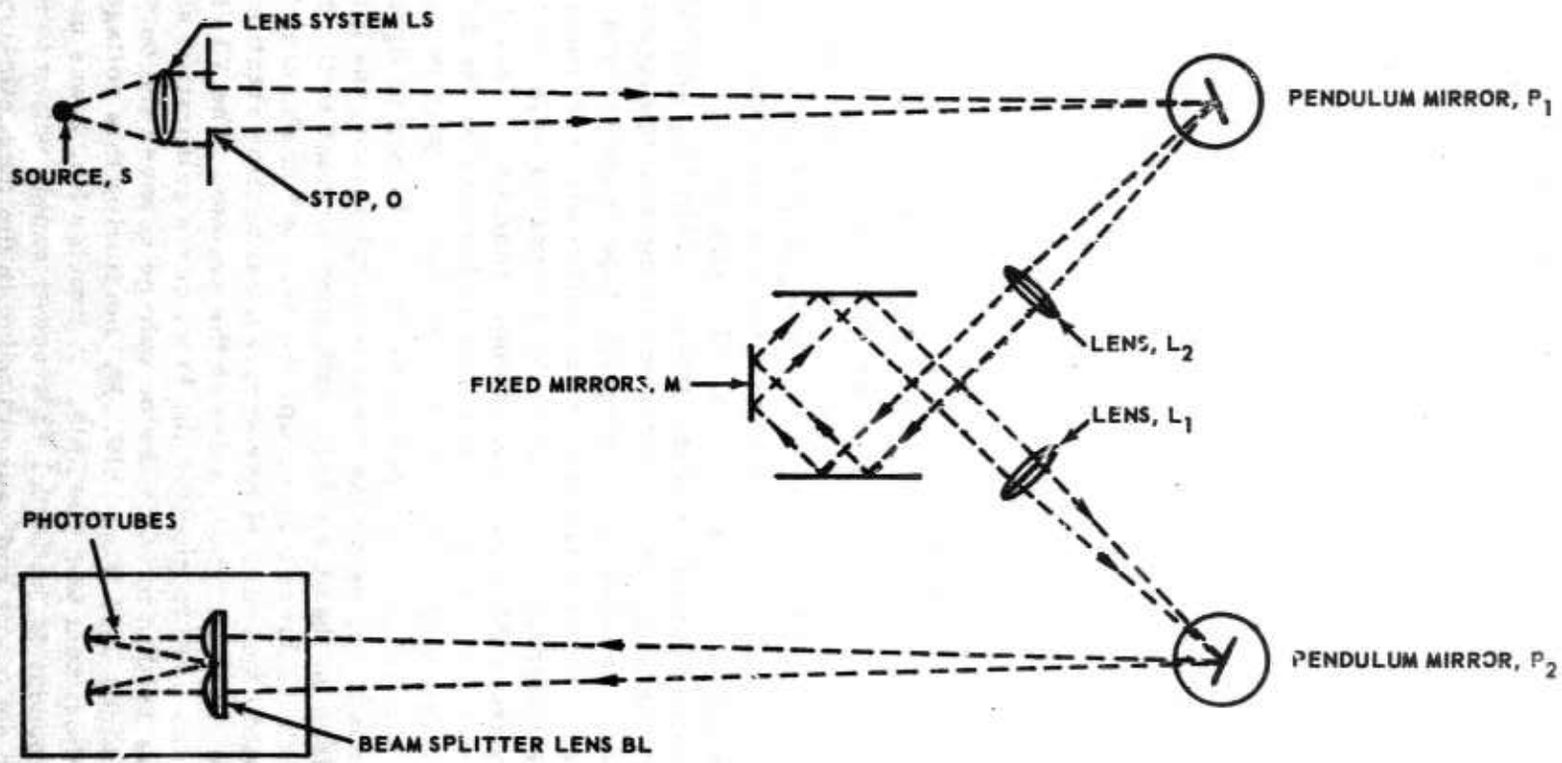

Figure 7. Ray diagram for torsion pendulum optical system

G 2364

The change from data acquisition to calibration and noise check was accomplished by inserting a large mirror in the optical path between the torsional pendulums and the light source. This mirror, as well as the other mirrors in the system, was flat to 1/4 wavelength and the lenses in the system were achromatic. A simplified sketch of the optical layout is shown in figure 8. The solid line indicates the optical path for the desired noise data and the broken line indicates the optical path during system static-noise checks and calibration. During system static-noise checks the input to the test galvanometer was effectively shorted and the resulting system output was caused by excess noise. This check was performed routinely to insure that excess noise was not of sufficient magnitude to cause errors. To calibrate the system, a low-level input was fed to the test galvanometer, which had been previously calibrated, and the resulting signal was recorded. From this information system calibration in output-voltage-per-unit-rotation was obtained. The complete optical system is shown in figure 9.

As stated, the experiment was designed so that data acquisition, calibration and noise checks were conducted without entering the pier room. These operations were accomplished using the equipment configuration shown in figure 10. Data from the phototube deck assembly, either test data or calibration data depending upon the position of the large mirror, were fed into the Model 4304 power supply in a balanced configuration. The output of the Model 4304 power supply, a single-ended cathode follower, was connected to the two input terminals of the signal conditioning amplifier. The signal-conditioning amplifier was an engineering unit built around commercially available solid-state operational amplifiers. Utilizing the available gain flexibility and low output impedance of the signal conditioning amplifier, the data were then fed to the strip-chart recorder and the analog magnetic-tape recorder. The monitor channel on the magnetic-tape recorder was used to examine the recorded data simultaneous (3 sec delay) with recording. The monitored data were recorded on the strip-chart recorder adjacent to the data coming directly from the signal-conditioning amplifier. This dual recording on the strip-chart recorder was done to insure that the data were being faithfully recorded by the magnetic-tape recorder. With the large mirror in the down position, corresponding to the solid lines in figure 8, test data were recorded. By using the motor-control switch, the large mirror could be raised so that the optical path corresponded to the dashed line in figure 8. With the large mirror up, the decade box shunting the calibration lines could be used to either supply a calibration rotation to the optical system or to check the static noise in the system. The VTVM in the calibration circuit was used to monitor the level of the calibration signal. Voltmeter No. 1 was used to monitor the dc voltage between the output-tube cathodes of the phototube deck assembly. By monitoring this voltage, effective control of optical adjustment was possible. Voltmeter No. 2 was used to monitor the dc component of the Model 4304 power supply output to insure that excessive offset did not occur and cause clipping in the magnetic-tape recorder.

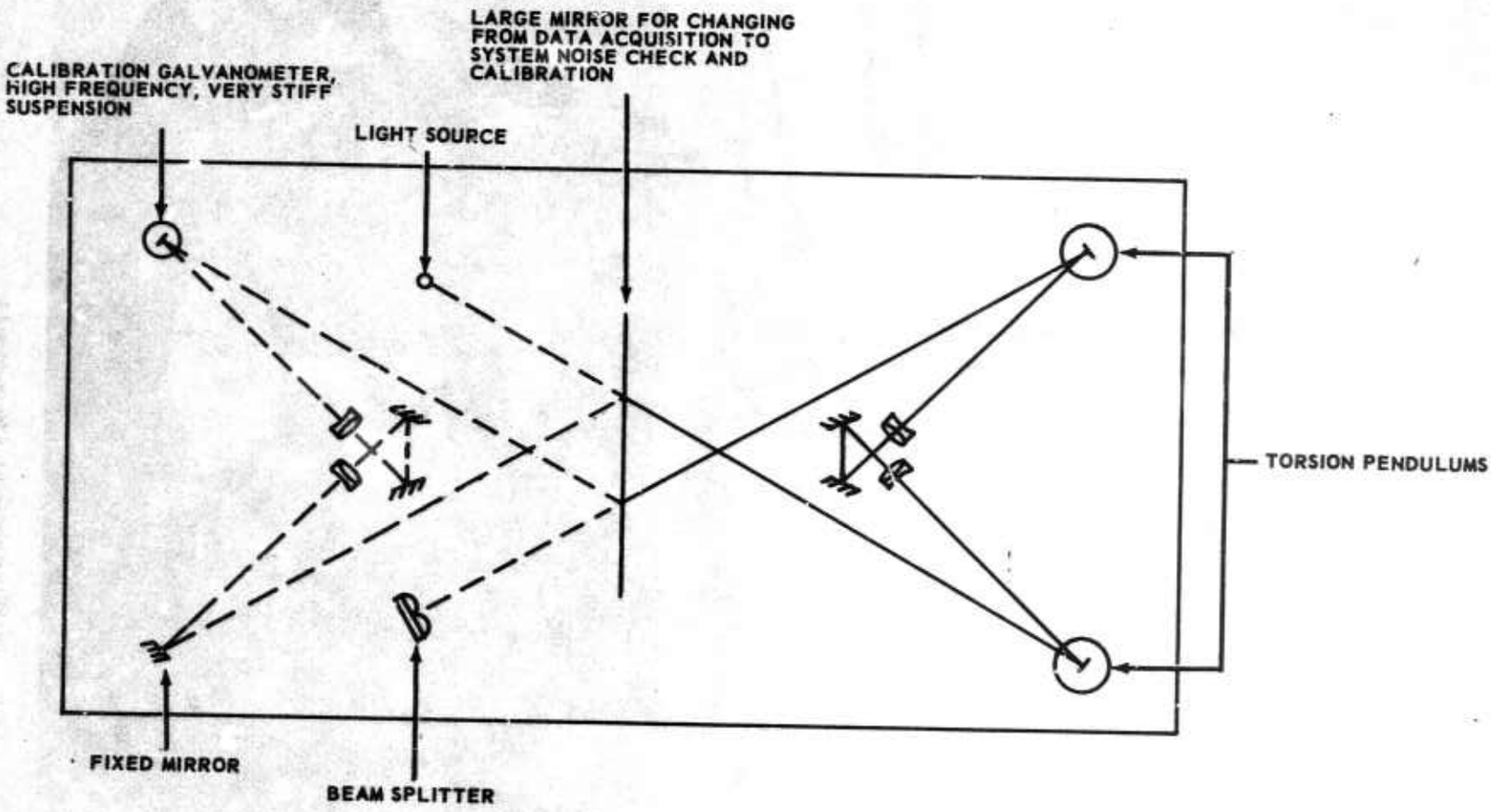

Figure 8. Optical layout

G 2365

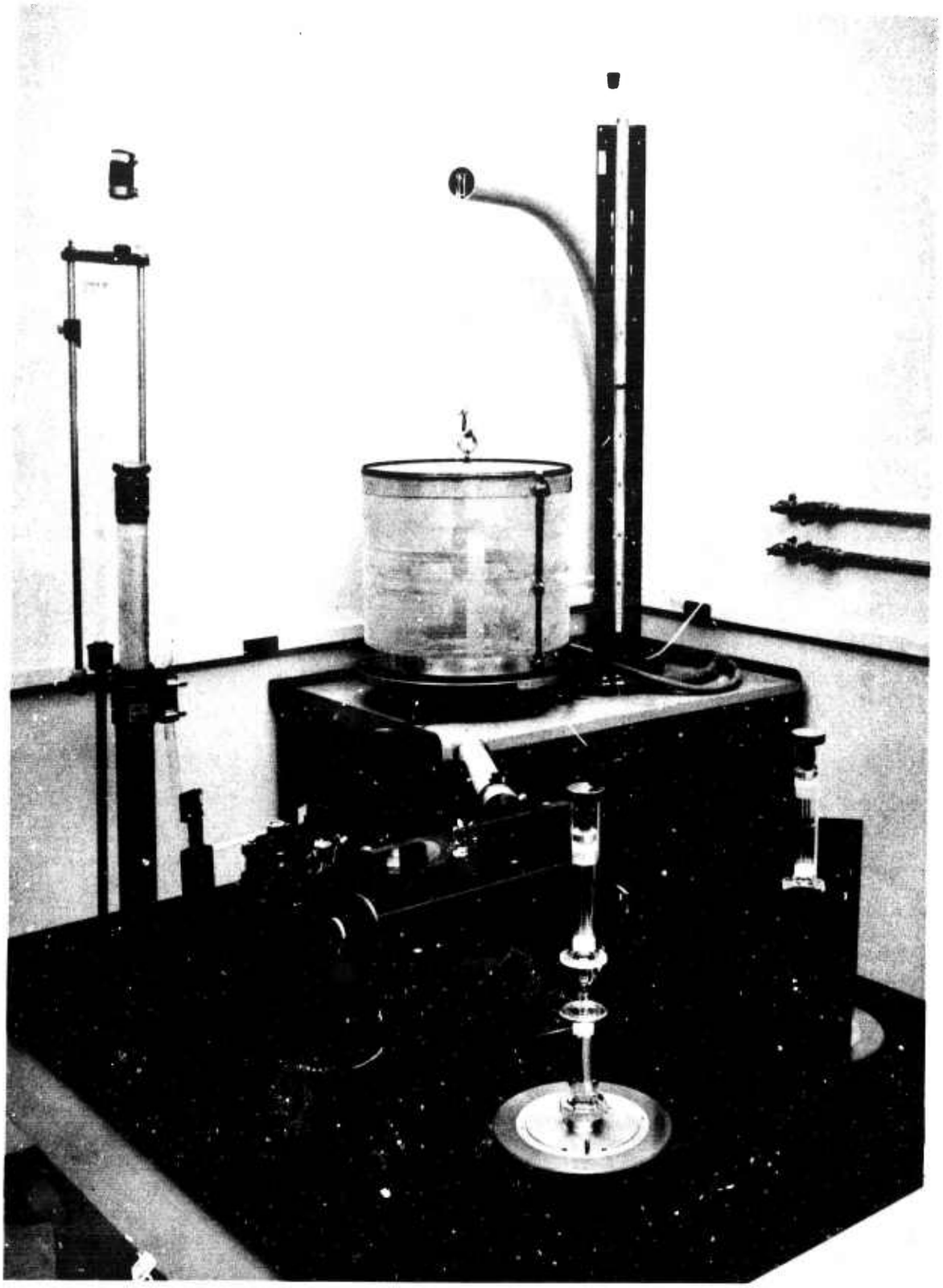

Figure 9. Optical system set up for experiment 1

G 1684

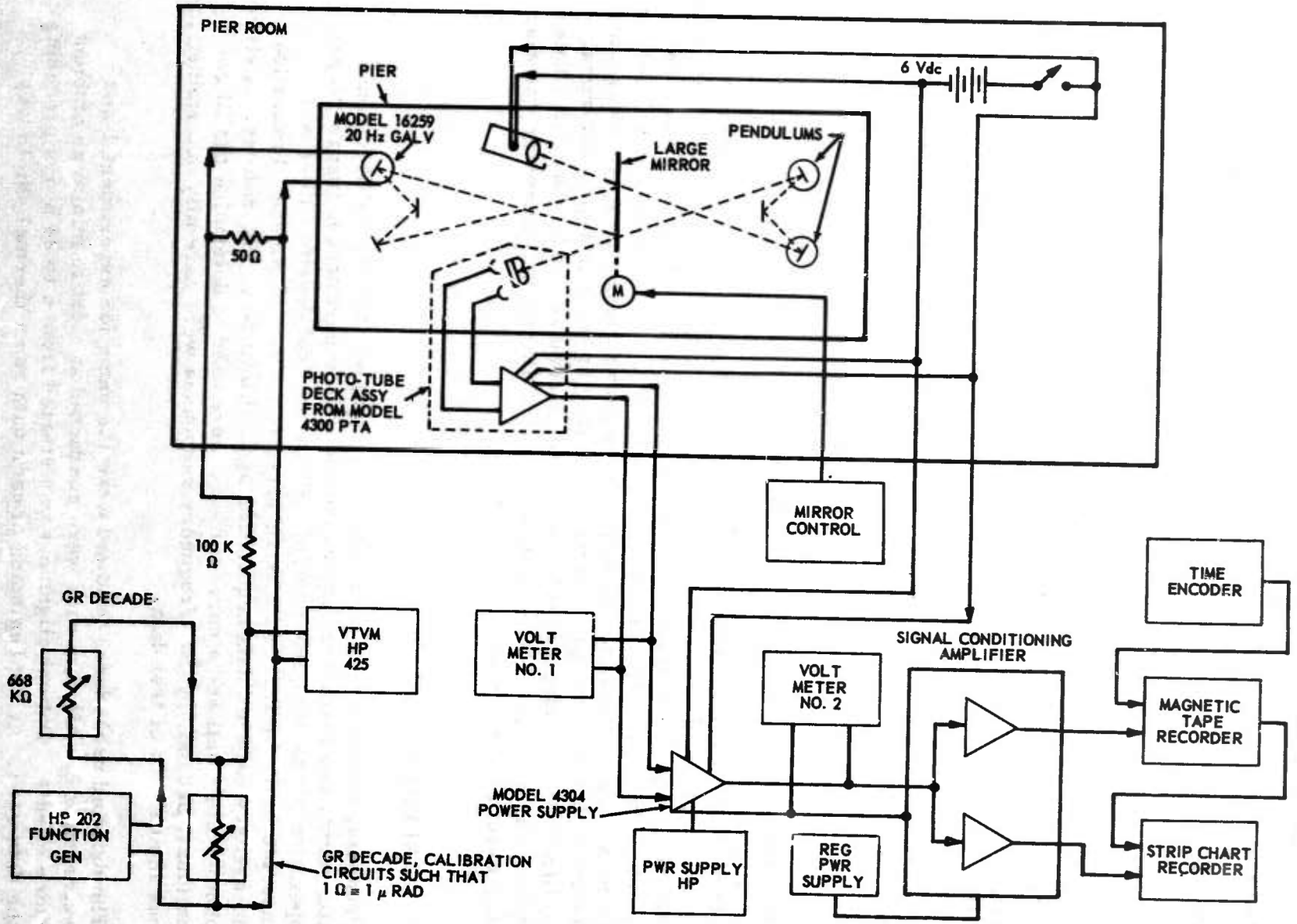

Figure 10. Block diagram of test setup for experiment 1

G 2367

3.2.2 Experiment 2

The torsion pendulums used in experiment 2 consisted of 2 galvanometers, 1 experimental and 1 Model 8530-1 galvanometer. The experimental galvanometer for experiment 2 was designed to match the Harris galvanometer such that the "response" of the combination would be similar to the response of a typical seismometer-galvanometer combination. The Harris galvanometer represented the seismometer in the combination and the special galvanometer was the galvanometer of the combination.

The Harris galvanometer had a natural period of 113 sec and the special galvanometer had a natural period of 10 sec. Experiment 2 required most of the equipment and apparatus used in experiment 1. The only significant difference was, of course, the test pendulums. Experiment 2 was not designed to include the cancelling technique utilized in experiment 1. Therefore, referring to figure 1, where changes in the system are shown in red, 1 torsion pendulum was replaced with the experimental galvanometer and 1 torsion pendulum was replaced with a fixed mirror.

The experimental galvanometer shown in figure 12 was built in a sealed housing like those used for the torsion pendulums. Because an identical pair of galvanometers was not required for experiment 2, considerable flexibility of design and assembly existed with regard to geometry, materials, and configuration. Considerable effort was therefore expended to achieve armature balance. The armature is shown in more detail in figure 13 where the balancing material can be seen. Also shown clearly in figure 13 are the electrical leads of the galvanometer. A pair of leads in a glass-to-metal seal from an incandescent bulb were inserted and sealed by epoxy in a hole in the side of the galvanometer housing. The Harris galvanometer was also very carefully balanced.

3.3 EXPERIMENTAL PROCEDURES

Preceding acquisition of data, and after complete optical and electronic alignment, two tests were conducted for each experiment to insure proper operation of the complete system. First, neutral density filters were inserted in the optical paths as required to prevent phototube illumination differences between data acquisition and calibration configurations. A silicon photo-voltaic cell and a current meter were used to determine the illuminations. Second, system frequency responses were carefully determined for use in analysis of test data.

The detailed procedures followed were the same for experiment 1 and experiment 2. All data runs were conducted at night to minimize ambient noise effects. Optical alignment was started from 6 to 24 hours preceding the data runs. At the beginning of each data run a thermal shield was

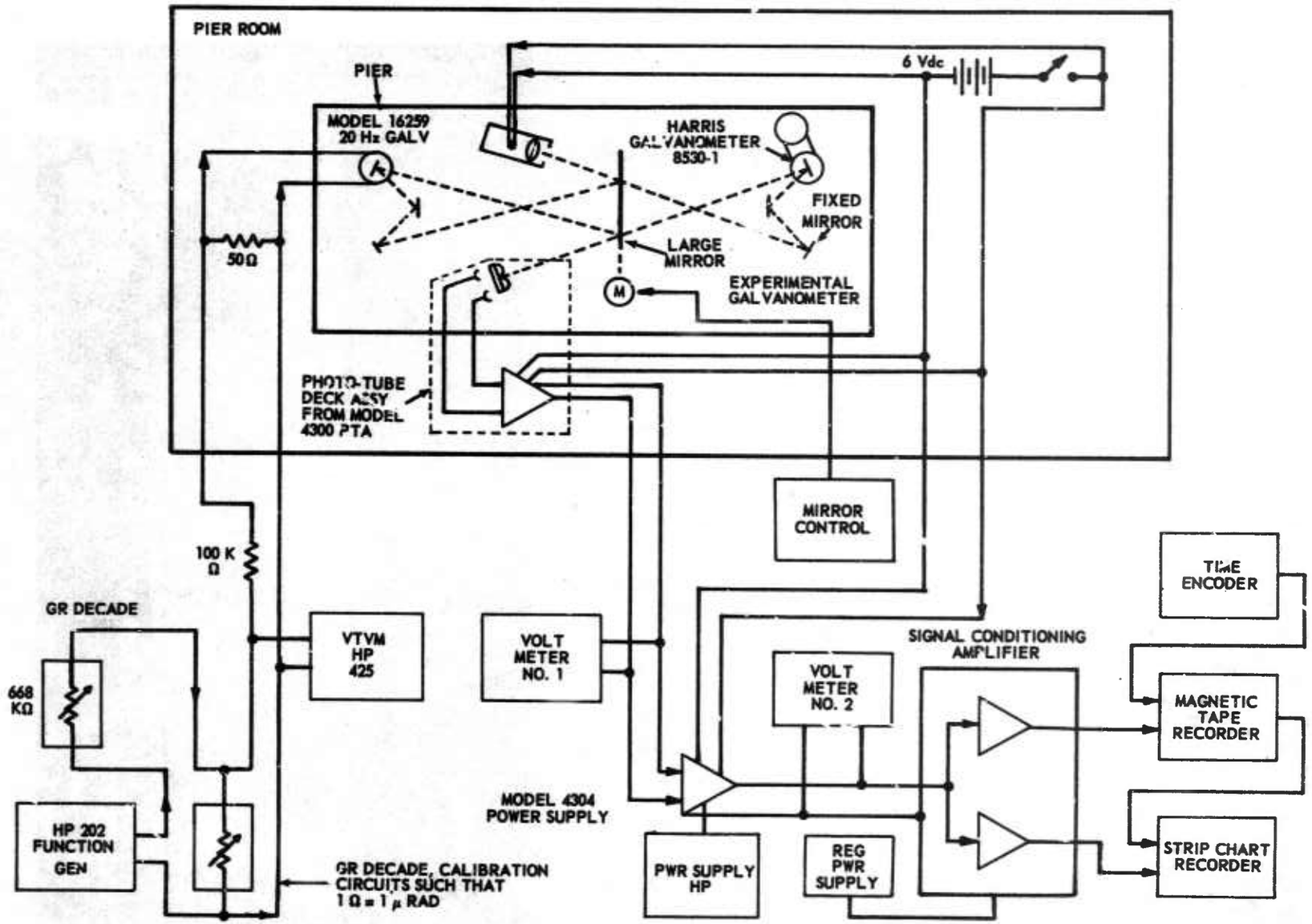

Figure 11. Block diagram of test setup for experiment 2

G 2368

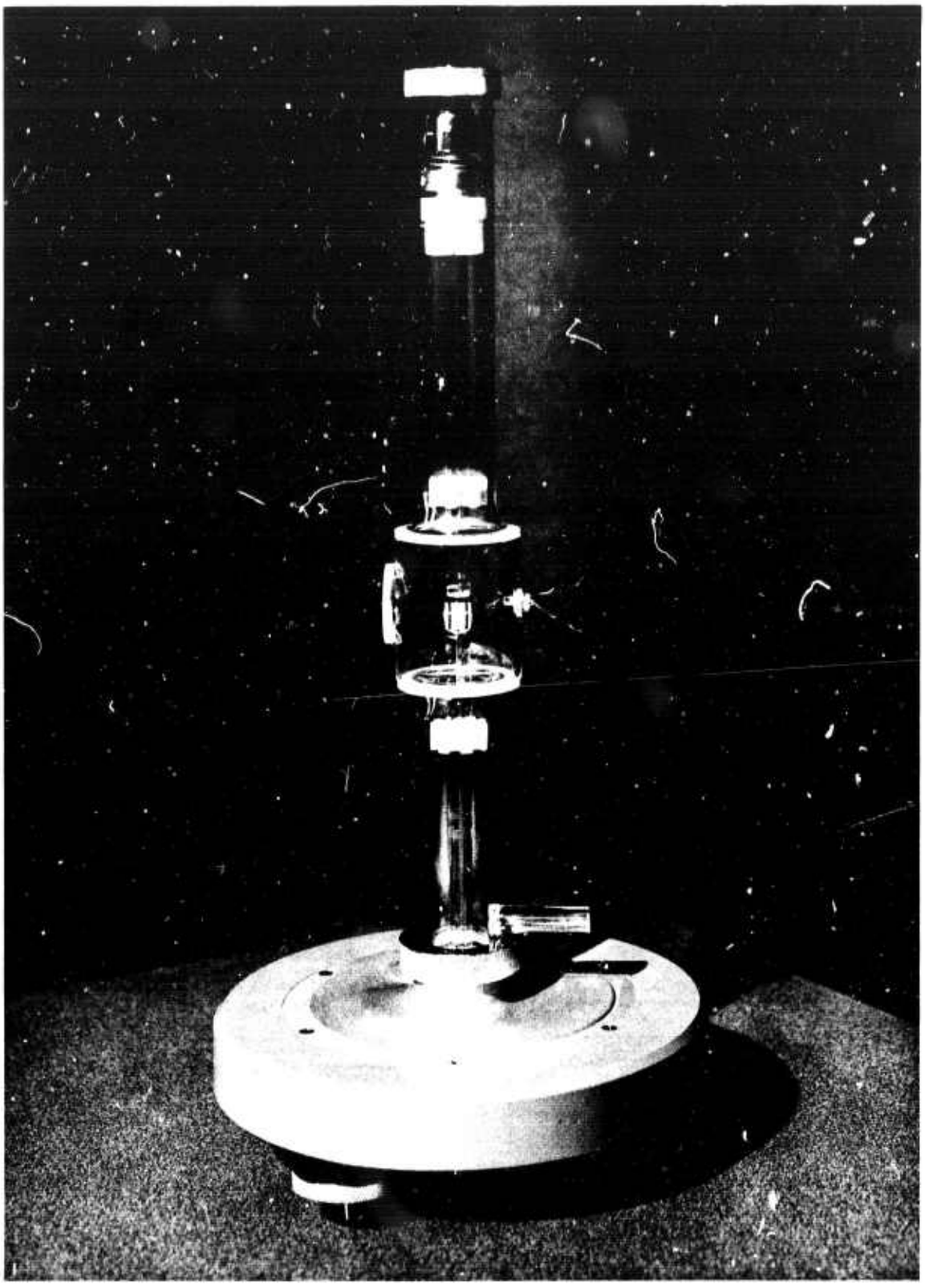

Figure 12. Experimental galvanometer used in experiment 2

G 2369

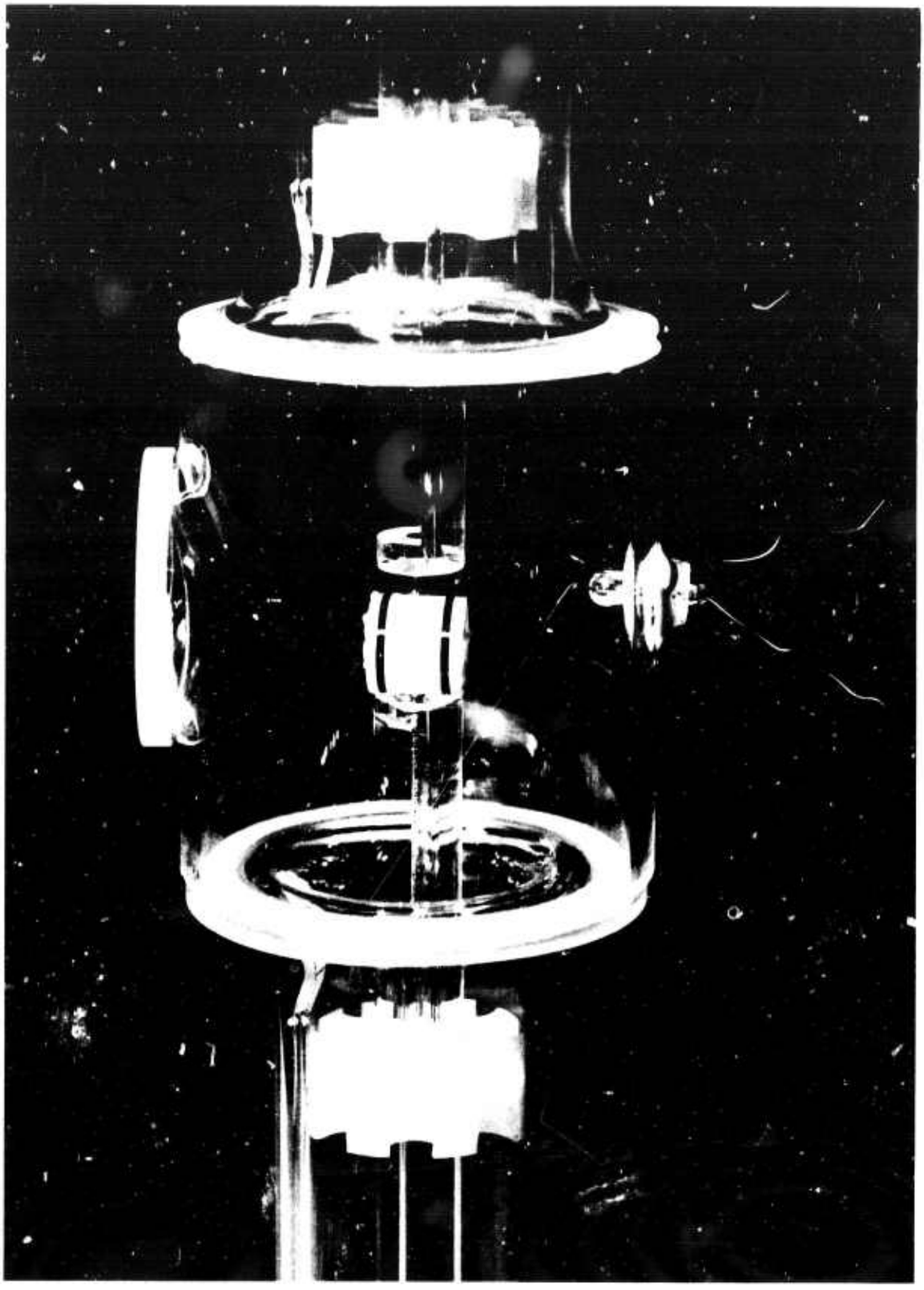

Figure 13. Close up of experimental galvanometer showing armature and electrical connections

G 2370

placed over the apparatus on the pier as shown in figure 14. After starting the alignment, the pier room was entered only to make necessary system adjustments. All electronic equipment was turned on a minimum of 1 hour before starting a data run. As much equipment as possible (all except that which was battery powered) was left on all the time. After optical and electronic adjustment and stabilization was completed, voltmeter No. 1 and voltmeter No. 2 were used to facilitate very fine adjustment of the complete system. The phototube deck assembly and the Model 4304 power supply were linear for a 30-volt p-p output from the power supply. Therefore, a reading between ±10 volts on voltmeter No. 1 was established as within a proper range of operation. Even though any point between ±10 volts was considered a satisfactory zero point, the zero point difference between data acquisition and calibration was made as small as possible. Next, the ZERO ADJUST control on the Model 4304 power supply was adjusted for a dc offset between ±0.1 volt. The recorders and signal-conditioning amplifier were then adjusted for convenient recording levels. At this point, the complete system was considered operating and completely adjusted.

The large mirror was then remotely inserted in the optical paths and a 5μ radian p-p deflection with a 10-second period was injected. This calibration signal was recorded for several minutes. The large mirror was then lowered and the acquisition of test data was accomplished.

Data runs were conducted for 5 different sets of conditions including two for which the air pressure in the pendulums was reduced to less than 10^{-1} mm of mercury. The reduced air pressure tests were conducted to determine the effects of air damping on the thermal noise spectra of systems that are largely damped electromagnetically.

Static noise check

a. Data was acquired with the large mirror remaining up throughout the run.

Experiment 1

b. $\gamma = 10.5$ sec
$\lambda_g = 0.26$
$\lambda_\theta = 0.01$

c. $\gamma = 10.5$ sec
$\lambda_g = 0.26$
$\lambda_\theta \ll 0.01$

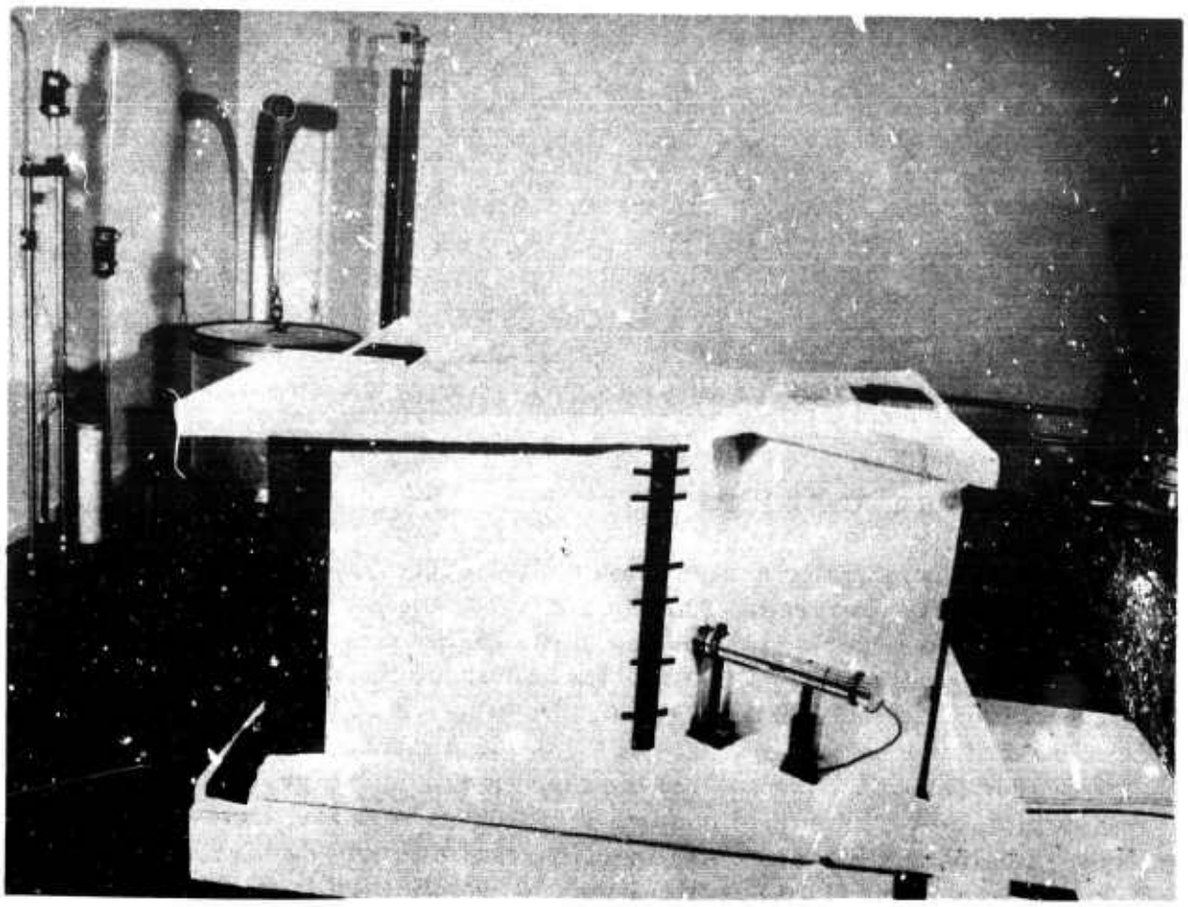

Figure 14. Optical system covered with insulating shield

G 2371

Experiment 2

d.	γ_g	=	10 sec	γ_o	=	113 sec
	λ_g	=	1.48	λ_o	=	0.67
	λ_θ	=	0.02	λ_x	=	0.33
e.	γ_g	=	10 sec	γ_o	=	113 sec
	λ_g	=	1.48	λ_o	=	0.67
	λ_θ	$\ll$	0.02	λ_x	=	0.33

4. EXPERIMENTAL RESULTS

4.1 ANALYSIS TECHNIQUES

All data were spectrally analyzed on a CDC 3100 Compute using the BLACKY spectral analysis program. Before analysis, the data were digitized at a rate of 4 samples per second. The digitizing process included analog band pass filtering with 3 dB points at 1 Hz and 0.002 Hz. The rolloff rate was 12 dB/octave above 1 Hz and 6 dB/octave below 0.002 Hz. Each data run consisted of at least 12,000 samples. After digitizing, each data run was reproduced through a digital-analog converter and the resulting analog record was compared to the corresponding strip-chart record. This comparison assured valid digital data. All spectra resulted from data segments 4000 samples long (maximum practical length) which were lagged 400 times by the analysis program. The spectral plots shown in sections 4.3 and 4.4 show each of the three 4000 sample segments and an average of the three.

4.2 STATIC NOISE CHECK

An example of system static noise is shown in figure 15. The spectrum of this noise is shown in the spectral curves to be introduced in sections 4.3 and 4.4.

4.3 EXPERIMENT 1

Typical analog data from experiment 1 is shown in figure 16. Figure 16a shows data for which the torsion pendulums were not evacuated, or $\lambda_\theta = 0.01$, and figure 16b shows data for which the torsion pendulums had been evacuated, or $\lambda_\theta \ll 0.01$. Spectra for the case where $\lambda_\theta = 0.01$ are

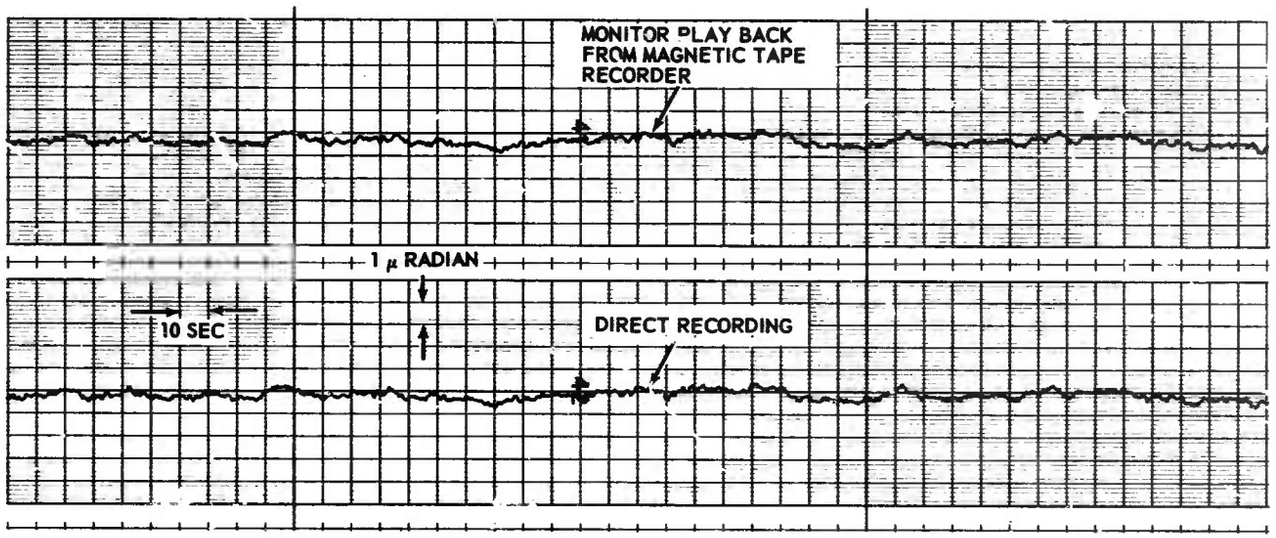

Figure 15. Data showing static noise level in system

G 2372

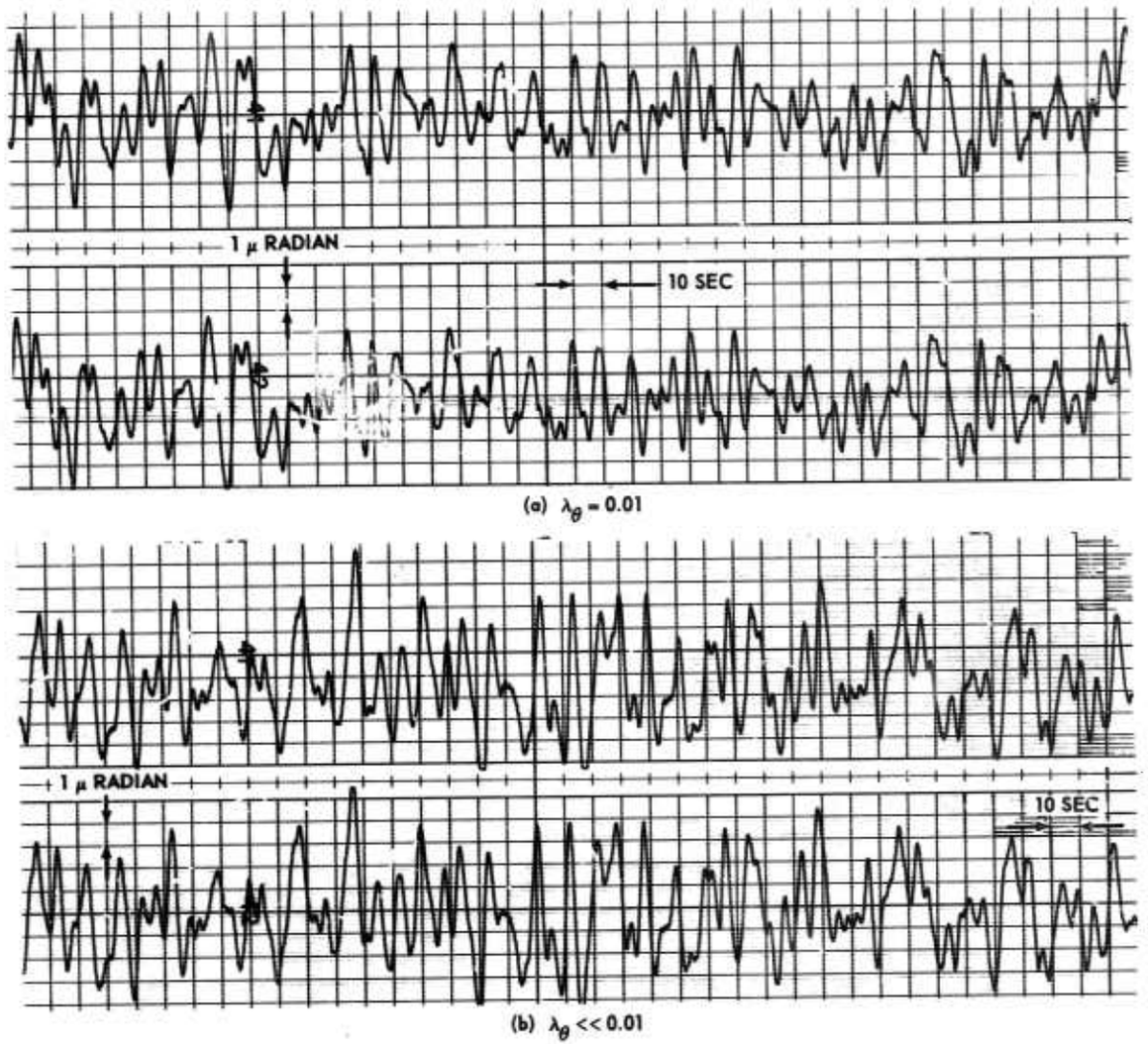

Figure 16. Data from experiment 1, galvanometer or seismometer connected to resistive load

G 2373

shown in figure 17 and for the case where $\lambda_\theta \ll 0.01$ are shown in figure 18. The data represented by figures 16a and 17 and by 16b and 18 were acquired on 2 different days.

4.4 EXPERIMENT 2

Analog data segments are shown in figure 19a for which the experimental galvanometer had not been evacuated and in figure 19b where the special galvanometer had been evacuated. Internal losses of the special galvanometer corresponding to figures 19a and 19b are $\lambda_\theta = 0.02$ and $\lambda_\theta \ll 0.02$, respectively. Spectra corresponding to figures 19a and 19b are figures 20 and 21, respectively. The data represented by figures 20 and 21 were acquired on 2 different days.

5. CONCLUSIONS

The theoretical equations generated by NBS seem quite reasonable when considering location of spectral peaks and total potential energy attributed by the equations to given seismometer-amplifier combinations.

Experiment 1 was considered to be only partially successful. Experiment 1 spectra, figures 17 and 18 contained components not predicted by theory. Lines are apparent in the spectra between 5 and 10 sec and between 15 and 20 sec. These components are considered to be lines in earth motion spectra and are considered to have caused responding motion in the torsion pendulums. Very slight imbalances in the pendulum armature(s) are the probable causes of the undesired pendulum motions. However, experiment 1 did not offer evidence to dispute the theory.

Experiment 2 was considered to be successful and agreement with theory was considered good. The data runs for which $\lambda_\theta = 0.01$ and $\lambda_\theta \ll 0.01$ resulted in very similar spectra. It can be concluded, as the theory predicts, that when $\lambda_\theta \ll \lambda_g$ or $\lambda_x \ll \lambda_\theta$ the Brownian motion contribution to the thermal energy of a galvanometer or seismometer is small and no significant improvement in performance will result from operating an instrument in an evacuated environment.

Based upon the NBS equations, the values of inertial mass given in section 2.2.2 are considered realistic. For the advanced long-period system to operate with magnifications as high as 130K the inertial mass of the seismometer should be at least 10 kg. For narrower portions of the system pass band, higher mangifications are possible if effective filtering, either in data acquisition or in data processing, can be provided. In order to operate

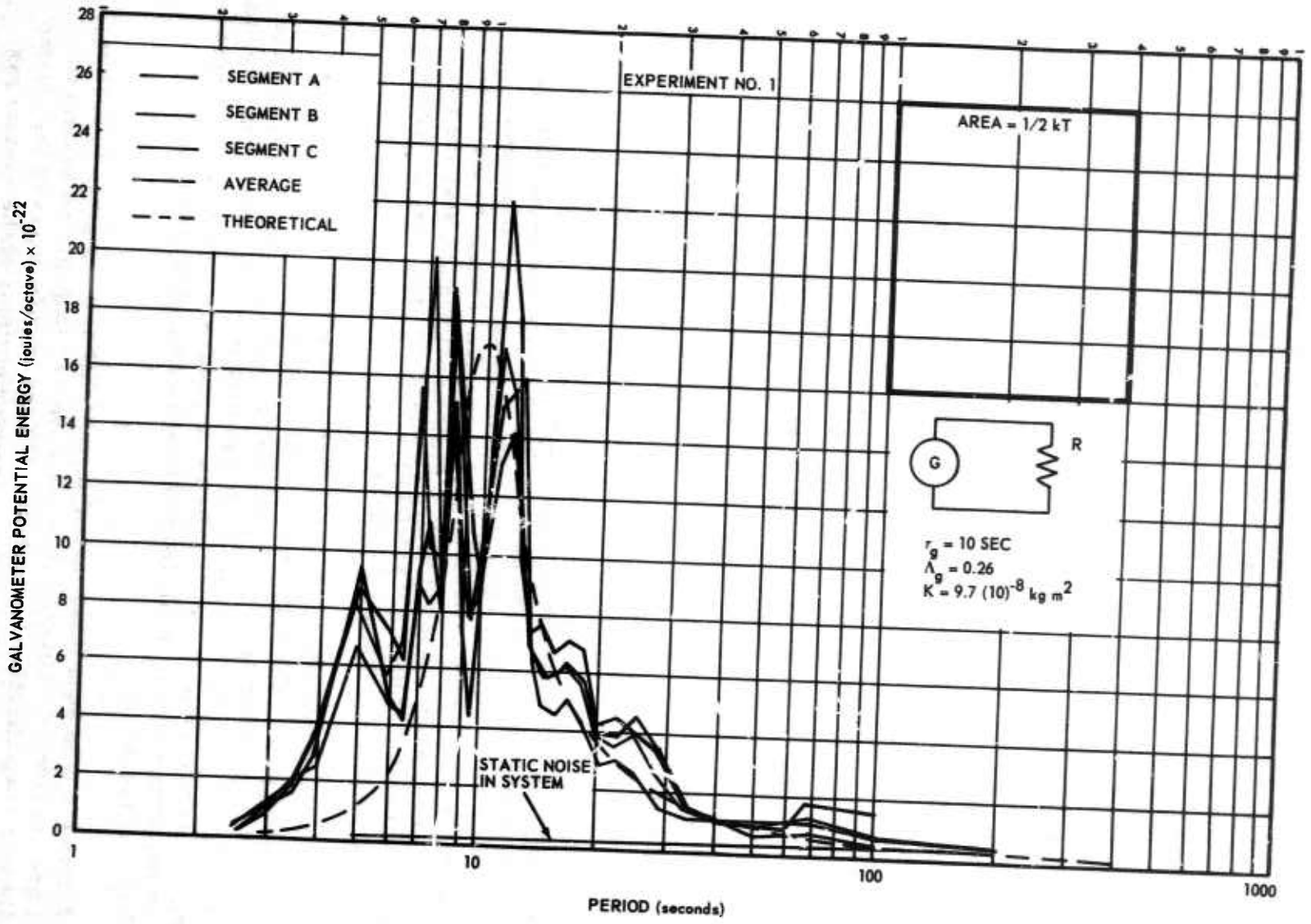

Figure 17. Spectra of experiment 1 data, λ_θ = 0.01

G 2374

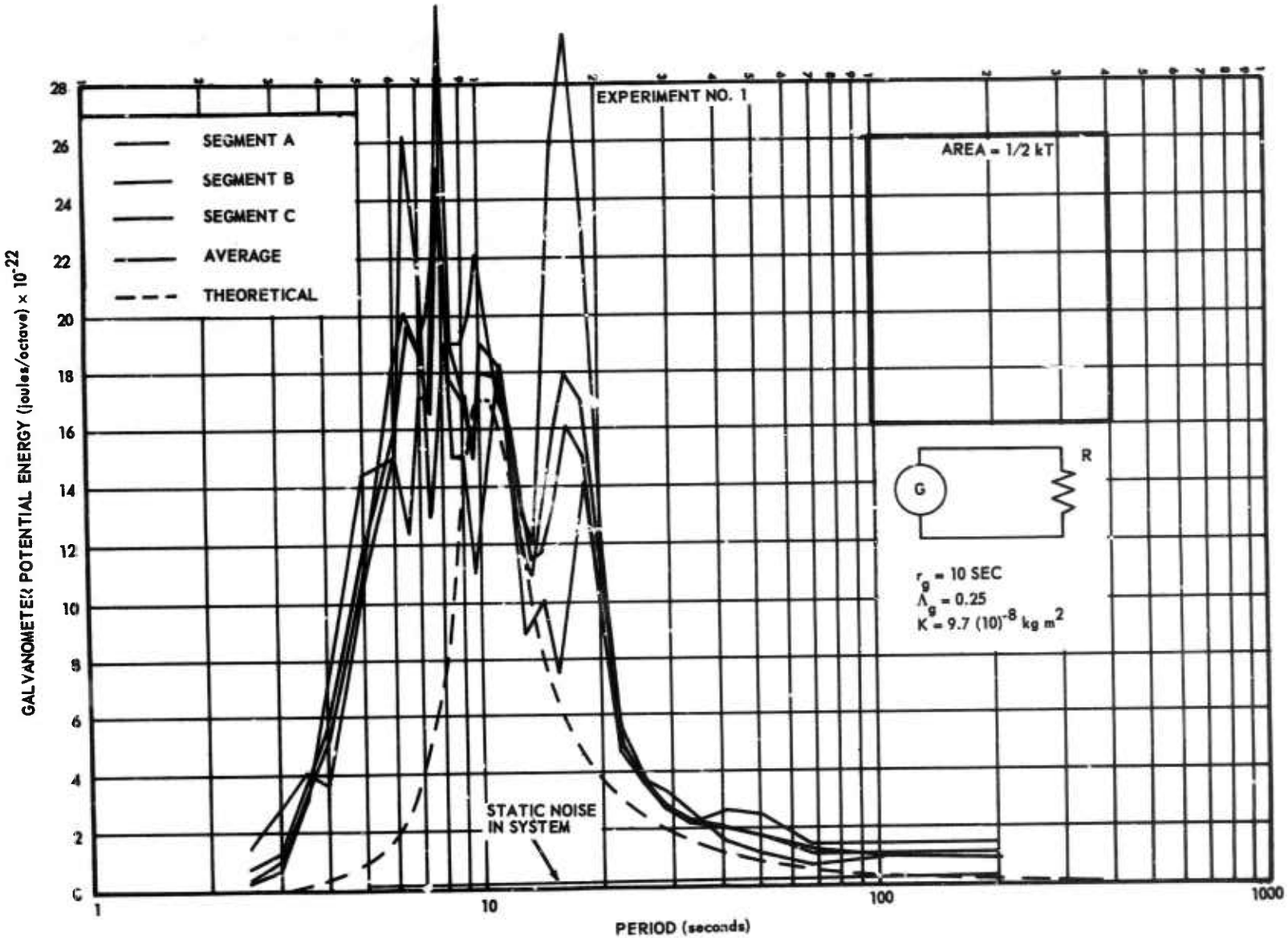

Figure 18. Spectra of experiment 1 data, $\theta_Y << 0.01$

G 2375

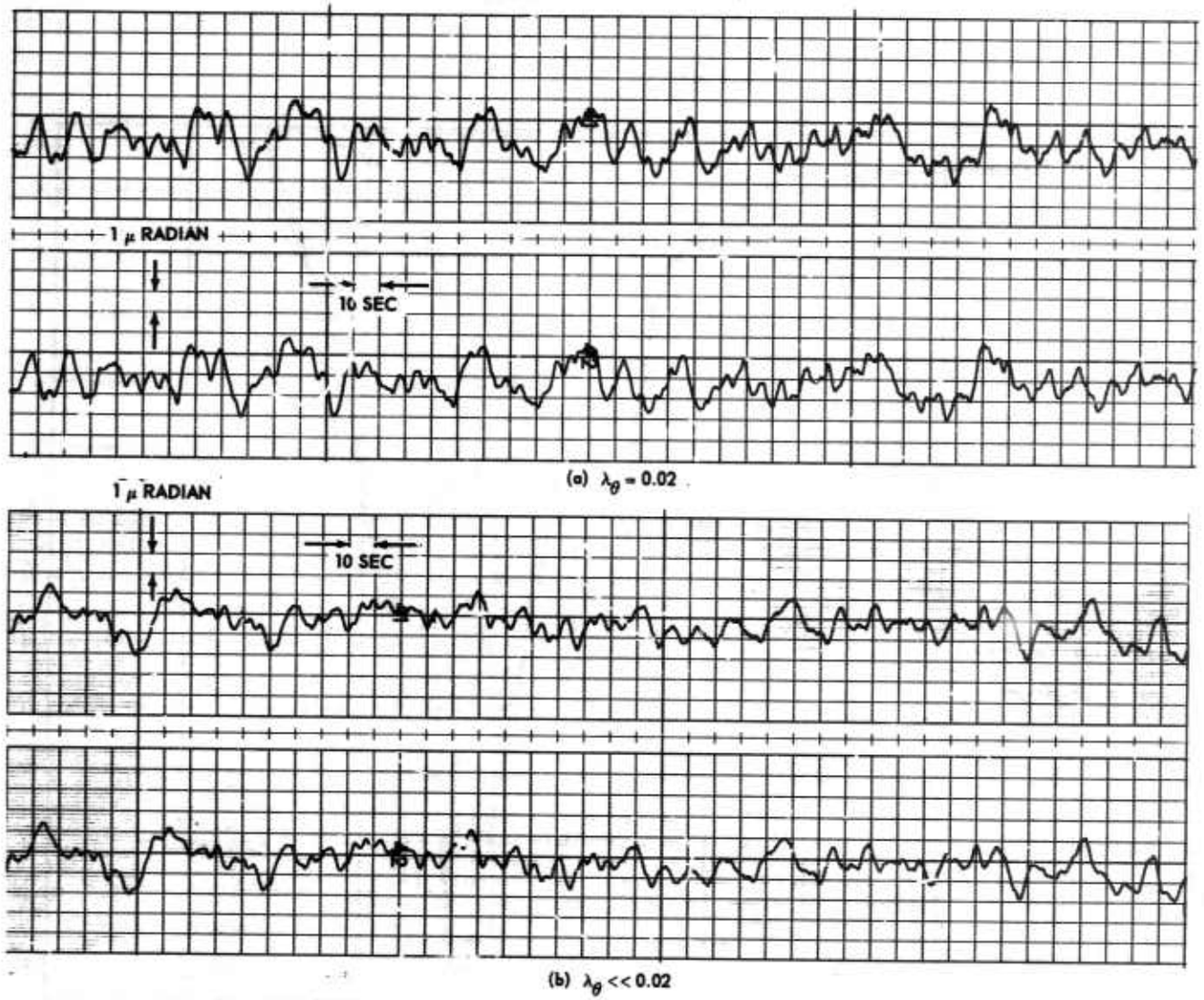

Figure 19. Reproduction of analog data sample from experiment 2, seismometer-galvanometer combination

G 2376

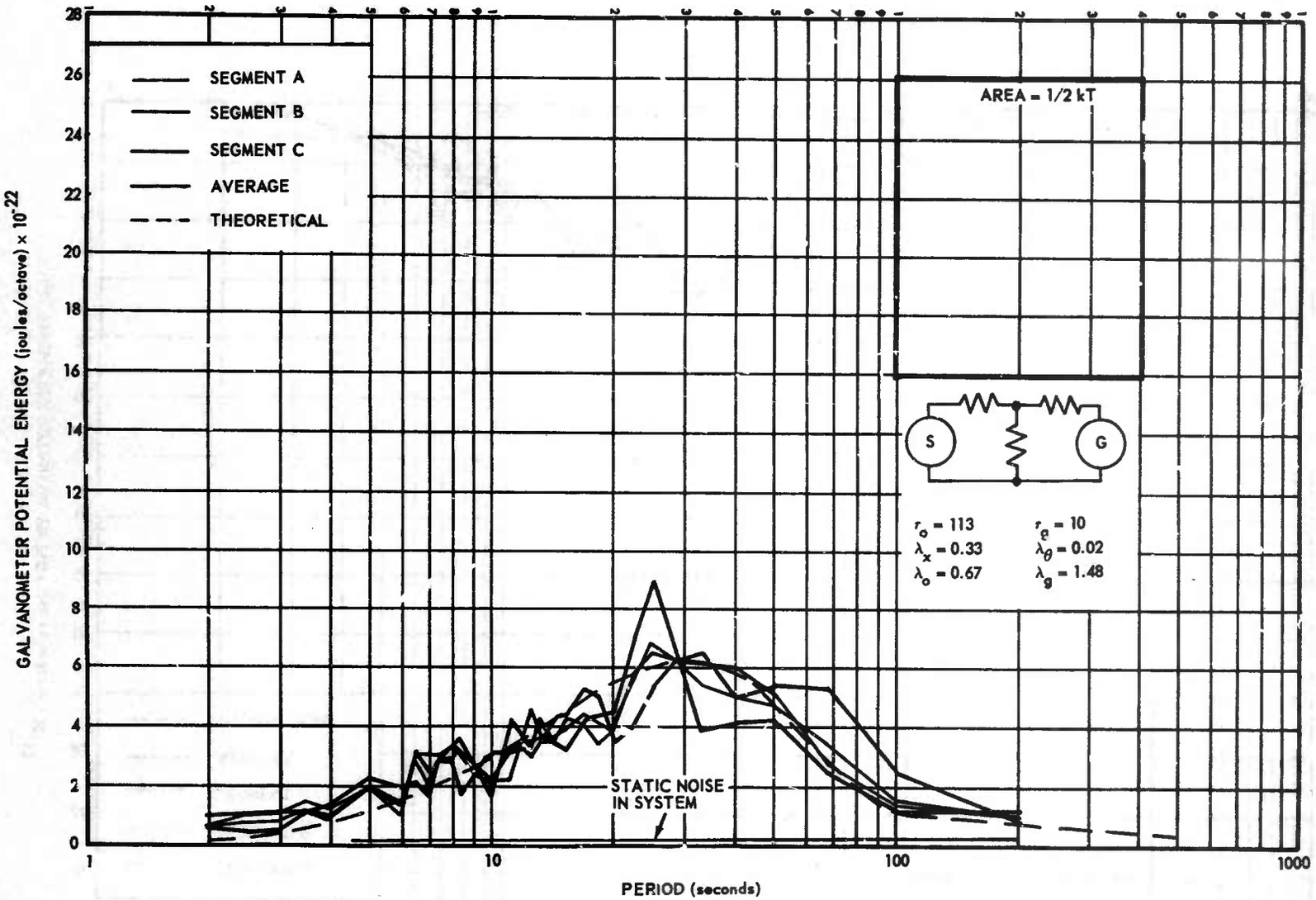

Figure 20. Spectra of experiment 2 data, λ_θ = 0.02

G 2377

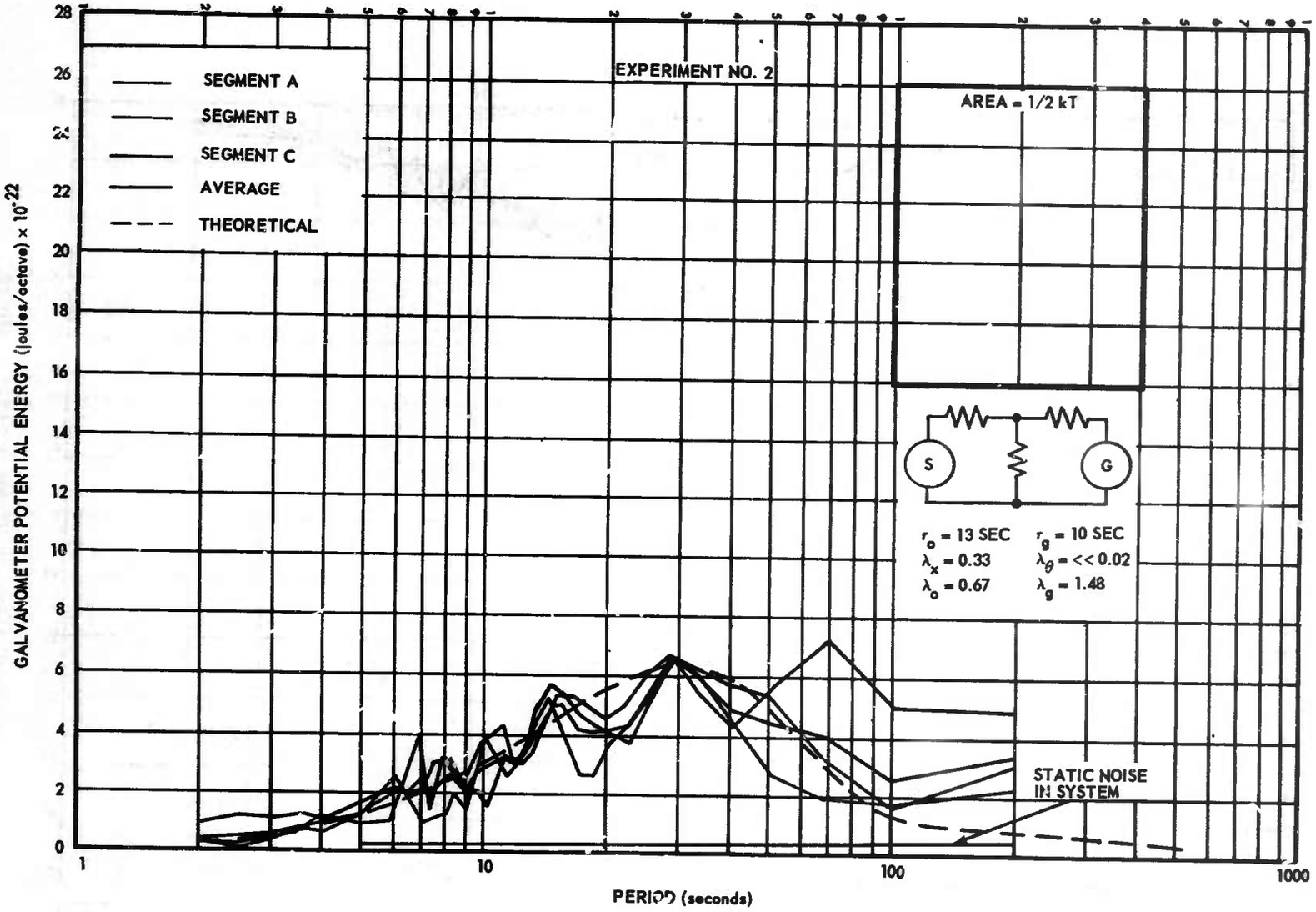

Figure 21. Spectra of experiment 2 data, λ_θ << 0.02

G 2378

the advanced long-period system at magnifications of 40K or 400K, the inertial mass of the seismometer must be 1 kg or 100 kg, respectively.

6. RECOMMENDATIONS

It is recommended that experiment 1 be repeated in a seismically quiet environment to complete the verification of the NBS theoretical analysis. It is also recommended that the site used be the Tonto Forest Seismological Observatory (TFSO) where the seismic background is low and well suited facilities exist. Isolated pier space is available at TFSO for the sensitive experimental instruments as is adequate laboratory space for the other electrical and vacumn equipment. Use of TFSO would result in the most economical repetition of the experiment without compromising the quality of the test results. If experiment 1 should be repeated it is anticipated that existing experimental equipment would be utilized, although it is probable that the torsion pendulums would be modified to further assure that seismic inputs would not affect the test results.

Until such time as other, more conclusively verified models are generated or unless the NBS theory is conclusively disproved, the NBS development should be considered valid. It is therefore recommended that the technique outlined in section 2.2.2 be considered valid for seismometer-galvanometer analyses.

It is further recommended that 10 kg be considered the minimum value of inertial mass for use in systems comparable to the advanced long-period system and which operate with magnifications up to 130K.

7. REFERENCES

Byrne, C. J., 1961, Instrument noise in seismometers, Bulletin of the Seismological Society of America, vol. 51, No. 1, pp. 69-84

McCoy, D. S., various reports on thermal noise written under Contracts AF 49(638)-1080 and AF 49(638)-1456

Johnson, J. B., 1928, Thermal agitation of electricity in conductors, Physical Review, vol. 32, pp. 97-109

Nyquist, H., 1928, Thermal agitation of electric charge in conductors, Physical Review, vol. 32, pp. 110-113

Barnes, R. B., and Silverman, S., 1934, Brownian motion as a natural limit to all measuring processes, Reviews of Modern Physics, vol. 6, p. 162

Milotz, J. and Zolingen, The Brownian Motion of Electrometers, Physics, vol. 19, p. 181

Landon, U. D., 1941, The distribution of amplitude with time in fluctuation noise, Proc T.R.E., February 1964, pp. 50-55

Matheson, H, and Gilbert, W., 1964, On the frequency distribution of Brownian motion (unpublished)

Johnson, D. P., and Matheson, H., 1962, An analysis of inertial seismometer-galvanometer combinations, NBS Report 7454, 182 p.

GLOSSARY OF TERMS

M	inertial mass of seismometer
K	moment of inertia of galvanometer armature
S	the stiffness of the mechanical spring in a seismometer
U	stiffness of the suspension of the galvanometer coil, the angular equivalent of S
G_1	the generator/motor constant associated with one real coil of the seismometer
G_3	the motor/generator constant of the galvanometer
r_x	losses within the instrument tending to reduce the velocity of the inertial mass such as residual eddy currents, air damping, etc. Presumed proportional to velocity.
r_θ	mechanical damping "constant" of the galvanometer. Usually chiefly air damping but would include losses due to eddy currents in a conducting coil form. The rotational equivalent of r_x.
C_x	The electrical capacity equivalent to the inertia of the bob in the electrical analog of the seismometer.
C_θ	The electrical capacity equivalent to the inertia of the armature in the electrical analog of the galvanometer.
L_x	The electrical numerically G_1^2/S inductance equivalent to the effective stiffness of the suspension in the electrical analog of a seismometer
L_θ	numerically $G^2{}_3/U$. The electrical inductance equivalent to the stiffness of the suspension of the galvanometer in the electrical analog.
R_s	The resistance of the shunt (common) arm of a resistive T pad connecting a seismometer to a galvanometer.
R_x	numerically G_1^2/r_x. The electrical resistance which is equivalent to the internal losses in the instrument in an electrical analog of the seismometer.

GLOSSARY OF TERMS, (Continued)

R_θ — numerically G^2_3/r_θ . The electrical resistance equivalent to the internal losses of the galvanometer in the electrical analog.

R_1 — the electrical resistance of the seismometer coil plus series resistance (if any).

R_3 — the electrical resistance of the galvanometer coil plus series resistance (if any).

α — the mean coupling coefficient, a measure of the attenuation provided by a resistive T pad.

R_o — $R_o \equiv G_1^2/2\omega_o M$. In a seismometer having negligible internal losses and negligible inductance this is the critical damping resistance (CDRX + coil resistance).

R_g — $R_g = G_3^2/2\omega_g K$. This is the critical damping resistance (CDRX plus coil resistance), of a galvanometer having no internal losses and negligible inductance.

ω_o — defines as $\sqrt{S/M}$, called the natural angular frequency, in radians per second, at which the inertial mass would oscillate after an impulse if it had no internal damping, when disconnected from an electrical circuit.

ω_g — natural angular frequency of a galvanometer, defines as $\sqrt{U/K}$.

ω — 2π times frequency in cps, angular frequency, frequency of a sinusoidal variable in radians per second.

θ — angular position of a galvanometer coil with respect to the case. The rotational equivalent of x.

y — earth displacement parallel to the motional axis of the instrument. For vertical instrument y is taken positive upward. The linear equivalent of θ .

λ_o — fraction of critical damping, or ratio to critical damping, of the seismometer due to the circuit resistance as seen by the seismometer (includes coil resistance of the seismometer).

λ_g — fraction of critical damping, or ratio to critical damping, of the galvanometer due to the circuit resistance as seen by the galvanometer (includes coil resistance).

GLOSSARY OF TERMS, (Continued)

R_θ numerically G^2_3/r_θ . The electrical resistance equivalent to the internal losses of the galvanometer in the electrical analog.

R_1 the electrical resistance of the seismometer coil plus series resistance (if any).

R_3 the electrical resistance of the galvanometer coil plus series resistance (if any).

α the mean coupling coefficient, a measure of the attenuation provided by a resistive T pad.

R_o $R_o \equiv G_1^2/2\omega_o M$. In a seismometer having negligible internal losses and negligible inductance this is the critical damping resistance (CDRX + coil resistance).

R_g $R_g = G_3^2/2\omega_g K$. This is the critical damping resistance (CDRX plus coil resistance), of a galvanometer having no internal losses and negligible inductance.

ω_o defines as $\sqrt{S/M}$, called the natural angular frequency, in radians per second, at which the inertial mass would oscillate after an impulse if it had no internal damping, when disconnected from an electrical circuit.

ω_g natural angular frequency of a galvanometer, defines as $\sqrt{U/K}$.

ω 2π times frequency in cps, angular frequency, frequency of a sinusoidal variable in radians per second.

θ angular position of a galvanometer coil with respect to the case. The rotational equivalent of x.

y earth displacement parallel to the motional axis of the instrument. For vertical instrument y is taken positive upward. The linear equivalent of θ .

λ_o fraction of critical damping, or ratio to critical damping, of the seismometer due to the circuit resistance as seen by the seismometer (includes coil resistance of the seismometer).

λ_g fraction of critical damping, or ratio to critical damping, of the galvanometer due to the circuit resistance as seen by the galvanometer (includes coil resistance).

GLOSSARY OF TERMS (Continued)

λ_x — fraction of critical damping, or ratio to critical damping, of a seismometer due to losses within the instrument tending to reduce the velocity of the inertial mass such as residual eddy currents, air damping, etc. Losses presumed proportional to velocity.

λ_θ — fraction of critical damping, or ratio to critical damping, of a galvanometer due to losses within the instrument tending to reduce the velocity of the inertial mass such as residual eddy currents, air damping, etc. Losses presumed proportional to velocity.

Λ_g — total galvanometer ratio to critical damping, where $\Lambda_g = \lambda_g + \lambda_\theta$

Λ_o — total seismometer ratio to critical damping, where $\Lambda_o = \lambda_o + \lambda_x$

Λ_m — geometric mean of total dampings, where $\Lambda_m = \sqrt{\Lambda_o \Lambda_g}$

ω_m — geometric mean of instrument natural frequencies, where $\omega_m = \sqrt{\omega_o \omega_g}$

γ — period in seconds

UNCLASSIFIED
Security Classification

DOCUMENT CONTROL DATA - R&D

(Security classification of title, body of abstract and indexing annotation must be entered when the overall report is classified)

1. ORIGINATING ACTIVITY (Corporate author)
Teledyne Industries, Geotech Division
3401 Shiloh Road
Garland, Texas

2a. REPORT SECURITY CLASSIFICATION
UNCLASSIFIED

2b GROUP

3. REPORT TITLE
Experimental Investigation of Thermal Noise

4. DESCRIPTIVE NOTES (Type of report and inclusive dates)
Final Report, Task 1a, Project VT/6706

5. AUTHOR(S) (Last name, first name, initial)
Trott, Wayne

6. REPORT DATE
15 November 1966

7a. TOTAL NO. OF PAGES

7b. NO. OF REFS

8a. CONTRACT OR GRANT NO.
AF 33(657)-16406

b. PROJECT NO.
VELA T/6706

c.

d.

9a. ORIGINATOR'S REPORT NUMBER(S)
Technical Report No. 66-90

9b. OTHER REPORT NO(S) (Any other numbers that may be assigned this report)

10. AVAILABILITY/LIMITATION NOTICES
Qualified users may obtain copies of this report from DDC. This document is subject to special export controls and each transmittal to foreign governments or foreign nationals may be made only with prior approval of the Chief, AFTAC

11. SUPPLEMENTARY NOTES

12. SPONSORING MILITARY ACTIVITY
HQ USAF (AFTAC/VELA
Seismological Center)
Washington, D. C. 20333

13. ABSTRACT
The primary objective of the experimental investigation of thermal noise was to verify and apply an analysis derived by National Bureau of Standards which can spectrally describe thermal energy in seismographs. When applied to a typical, operational, long-period seismograph, the NBS analysis shows the need for 10 kg inertial mass for a system magnification of about 130 k at 25 sec. Two experiments were designed to verify the NBS analysis. The first experiment was conducted to determine and verify the thermal energy spectrum for a seismometer or galvanometer connected to a resistive load. As a result of excessive uncancelled seismic inputs, the first experiment was only partially successful. The second experiment was conducted to determine and verify the thermal energy spectrum of the galvanometer in a seismometer-galvanometer combination. The results of the second experiment were agreement with theory. There was sufficient agreement between the empirical and theoretical spectra to the validity of the NBS analysis. The NBS analysis was therefore recommended for present use, but repetition of the first experiment in a seismically quieter location was recommended to further verify the analysis. (U)

DD FORM 1 JAN 64 1473

UNCLASSIFIED
Security Classification

14. KEY WORDS	LINK A		LINK B		LINK C	
	ROLE	WT	ROLE	WT	ROLE	WT
Thermal noise VELA T/6706 VT/6706 Long-Period Seismograph Development						

INSTRUCTIONS

1. ORIGINATING ACTIVITY: Enter the name and address of the contractor, subcontractor, grantee, Department of Defense activity or other organization *(corporate author)* issuing the report.

2a. REPORT SECURITY CLASSIFICATION: Enter the overall security classification of the report. Indicate whether "Restricted Data" is included. Marking is to be in accordance with appropriate security regulations.

2b. GROUP: Automatic downgrading is specified in DoD Directive 5200.10 and Armed Forces Industrial Manual. Enter the group number. Also, when applicable, show that optional markings have been used for Group 3 and Group 4 as authorized.

3. REPORT TITLE: Enter the complete report title in all capital letters. Titles in all cases should be unclassified. If a meaningful title cannot be selected without classification, show title classification in all capitals in parenthesis immediately following the title.

4. DESCRIPTIVE NOTES: If appropriate, enter the type of report, e.g., interim, progress, summary, annual, or final. Give the inclusive dates when a specific reporting period is covered.

5. AUTHOR(S): Enter the name(s) of author(s) as shown on or in the report. Enter last name, first name, middle initial. If military, show rank and branch of service. The name of the principal author is an absolute minimum requirement.

6. REPORT DATE: Enter the date of the report as day, month, year; or month, year. If more than one date appears on the report, use date of publication.

7a. TOTAL NUMBER OF PAGES: The total page count should follow normal pagination procedures, i.e., enter the number of pages containing information.

7b. NUMBER OF REFERENCES: Enter the total number of references cited in the report.

8a. CONTRACT OR GRANT NUMBER: If appropriate, enter the applicable number of the contract or grant under which the report was written.

8b, 8c, & 8d. PROJECT NUMBER: Enter the appropriate military department identification, such as project number, subproject number, system numbers, task number, etc.

9a. ORIGINATOR'S REPORT NUMBER(S): Enter the official report number by which the document will be identified and controlled by the originating activity. This number must be unique to this report.

9b. OTHER REPORT NUMBER(S): If the report has been assigned any other report numbers *(either by the originator or by the sponsor)*, also enter this number(s).

10. AVAILABILITY/LIMITATION NOTICES: Enter any limitations on further dissemination of the report, other than those imposed by security classification, using standard statements such as:

(1) "Qualified requesters may obtain copies of this report from DDC."

(2) "Foreign announcement and dissemination of this report by DDC is not authorized."

(3) "U. S. Government agencies may obtain copies of this report directly from DDC. Other qualified DDC users shall request through

_____."

(4) "U. S. military agencies may obtain copies of this report directly from DDC. Other qualified users shall request through

_____."

(5) "All distribution of this report is controlled. Qualified DDC users shall request through

_____."

If the report has been furnished to the Office of Technical Services, Department of Commerce, for sale to the public, indicate this fact and enter the price, if known.

11. SUPPLEMENTARY NOTES: Use for additional explanatory notes.

12. SPONSORING MILITARY ACTIVITY: Enter the name of the departmental project office or laboratory sponsoring *(paying for)* the research and development. Include address.

13. ABSTRACT: Enter an abstract giving a brief and factual summary of the document indicative of the report, even though it may also appear elsewhere in the body of the technical report. If additional space is required, a continuation sheet shall be attached.

It is highly desirable that the abstract of classified reports be unclassified. Each paragraph of the abstract shall end with an indication of the military security classification of the information in the paragraph, represented as *(TS)*, *(S)*, *(C)*, or *(U)*.

There is no limitation on the length of the abstract. However, the suggested length is from 150 to 225 words.

14. KEY WORDS: Key words are technically meaningful terms or short phrases that characterize a report and may be used as index entries for cataloging the report. Key words must be selected so that no security classification is required. Identifiers, such as equipment model designation, trade name, military project code name, geographic location, may be used as key words but will be followed by an indication of technical context. The assignment of links, rules, and weights is optional.

GPO 666-551

APPENDIX 1 to TECHNICAL REPORT NO. 66-90

STATEMENT OF WORK

EXHIBIT "A"

STATEMENT OF WORK TO BE DONE

AFTAC Project Authorization No. VELA T/6706

11 MAR 1966

1. Tasks:

a. Experimental Investigation of Thermal Noise. Continue the experimental investigation, defined in Project VT/072, of thermal noise components in seismograph systems, using torsional pendulums and associated equipment available from that project. Determine experimentally the spectral distributions of thermal noise in seismograph systems and compare the experimental results with theoretical predictions, as those derived by the National Bureau of Standards, for example. Provide data and methods for determining the ultimate possible magnification of a seismograph. Work on this task is to be completed within 4 months of the initial authorization date.

b. Development of a Long-Period Triaxial Borehole Seismometer. Modify the "Melton" long-period triaxial seismometer developed under Project VT/072 to adapt it for routine operation in shallow (200-foot) boreholes. Reduce the seismometer's diameter so it will fit inside standard 13.375-inch outside diameter shallow-well casing. Develop and add a suitable level sensor and remotely-controlled levelling device.

c. Preliminary Testing of the Long-Period Triaxial Borehole Seismometer. Prepare a cased, shallow borehole at a VELA seismological observatory to be designated by the AFTAC project officer. Assemble handling equipment for installing the seismometer. Conduct preliminary tests of the modified instrument in the test hole to determine its stability and the effects of temperature and local tilting as functions of depth. Through the use of improved installation techniques, selective filtering, design improvement or other means, develop a method for operating the seismometer so that magnification in the 10 to 100 sec period band is limited only by propagating seismic noise.

d. Field Measurements with the Long-Period Triaxial Borehole Seismometer. Collect and analyze data to determine long-period signal and noise characteristics in shallow boreholes, to identify principal long-period seismic noise components, to ascertain depth-environmental effects, and to compare the performance of the triaxial borehole seismometer with standard long-period seismometers.

2. Data Requirements: Provide report as specified by DD Form 1423, with Attachment 1 thereto.

APPENDIX 2 to TECHNICAL REPORT NO. 66-90

ON THE FREQUENCY DISTRIBUTION OF BROWNIAN MOTION

ON THE FREQUENCY DISTRIBUTION OF BROWNIAN MOTION

By Harry Matheson & Walt Gilbert, NBS

Accepting the reasoning of Nyquist (Phys. Rev. 32, 110, July 1928) and using the nomenclature in NBS Report 7454, the following development can be obtained.

Figure 4.1 in NBS Report 7454 is reproduced here as figure 1 for convenient reference.

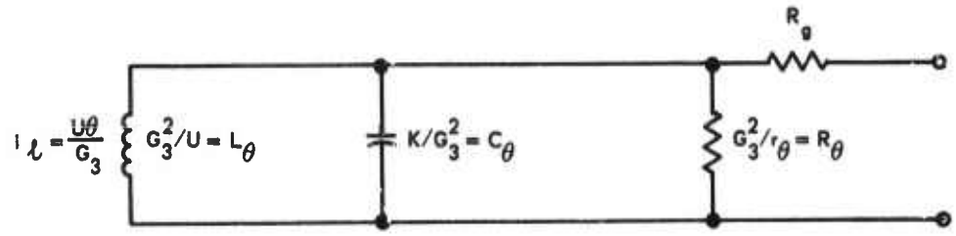

Figure 1. Electrical analog of a galvanometer

First the reader should note that in observing or recording the deflections of the galvanometer mirror from its average position he is observing a quantity proportional to the current through the inductor in the above circuit and the angular velocity of the mirror is proportional to the emf across the inductor.

The term r_θ was introduced in Report 7454 as the coefficient of a term representing energy losses within the instrument whether due to the visco-elastic properties of the suspension, eddy currents, or air damping. The galvanometers typically used in seismological work are constructed with suspensions having very little energy loss and these losses will

be neglected in what follows. These galvanometers are also usually designed to have minimal eddy current losses, and in what follows these also will be ignored. Air damping, or windage losses, have been simulated by the introduction of the virtual resistor R_θ, and insofar as these losses are strictly proportional to the angular velocity of the armature, this substitution is exact. For moderate deflections, this is a reasonable assumption; R_θ depends upon a shape factor of the armature and interior of the case as well as the viscosity of the contained fluid. For small deflections, those approaching the mean free path of the molecules of contained fluid, the motions of the armature are reduced by the presence of the fluid only part of the time. A significant fraction of the time, unbalanced impacts of the molecules will increase or decrease the kinetic or potential energy of the armature. Under these conditions, we will consider only the rms kinetic and potential energy of the armature and R_θ is a noisy resistor of the type considered by Nyquist in that it can both absorb power from the armature and feed power into the armature.

Considering R_θ as an ideal resistor in series with a zero resistance generator simulating the noise of the resistor, we can write

$$E_\theta = (i_\ell + i_c)\ R_\theta + i_\ell\, j\,\omega L_\theta \qquad (1)$$

where E_θ is the voltage of the generator, i_c is the current through the capacitor, and i_ℓ is the current through the inductor.

Since $i_c/i_\ell = -\omega^2/\omega_g^2$, $\omega_g^2 = 1/L_\theta C_\theta$, and $L_\theta = 2R_g/\omega_g$

equation (1) can be written

$$E_\theta = \left\{\left(\frac{\omega_g^2 - \omega^2}{\omega^2}\right) R_\theta + 2jR_g\,\omega/\omega_g\right\} i_\ell \qquad (2)$$

Expressing the internal losses of the instrument as a fraction of critical damping $\lambda_\theta = R_g/R_\theta$ noting that the quantity sought, θ, is related to i_ℓ by $i_\ell = \theta U/G_3$, and by using the substitution $G_3^2 = L_\theta U$, we can write

$$\frac{|E_\theta|^2}{R_\theta} = \left\{\left(\frac{\omega_g^2 - \omega^2}{\omega_g}\right)^2 + 4\lambda_\theta^2\,\omega^2\right\} \frac{U|\theta|^2}{2\lambda_\theta\,\omega_g} \qquad (3)$$

This equation relates galvanometer deflection to the noise in the damping resistor at any specific frequency. The potential energy in the galvanometer over an arbitrary frequency interval (1 to 2) is given by rewriting equation (3) in integral form.

$$\frac{U|\theta|^2}{2}\Bigg|_1^2 = \int_1^2 \frac{\lambda_\theta\,\omega_g^3}{(\omega_g^2 - \omega^2)^2 + 4\lambda_\theta^2\,\omega_g^2\,\omega^2} \cdot \frac{|E|^2}{R_\theta}\,df \qquad (4)$$

From the reasoning of Nyquist, we make the substitution $|E^2|/4R = kT$, and with algebraic manipulation this may be rewritten

$$\frac{U|\theta|^2}{2}\Bigg|_1^2 = \int_1^2 \frac{2\lambda_\theta}{(1 - x^2)^2 + 4\lambda_\theta^2\,x^2} \cdot \frac{kT}{\pi}\,dx \qquad (5)$$

Note that this equation is written in terms of the normalized frequency, $x = \omega / \omega_g$.

A necessary, but not sufficient, condition that this equation corresponds to the real spectral distribution is that over the range $\omega = o$ to $\omega = \infty$, the value of this integral be kT/2. Expanding and factoring the denominator it may be written as $(a^2 + x^2)\ (b^2 + x^2)$ where $a^2 b^2 = 1$ and $a^2 b^2 = 4\lambda_\theta^2 - 2$. From standard tables of integrals

$$\int_o^\infty \frac{dx}{(a^2 + x^2)\ (b^2 + x^2)} = \frac{\pi}{2\ ab\ (a + b)}$$

so that equation 5 integrates to

$$\frac{U|\theta|^2}{2}\Bigg|_o^\infty = \frac{2\lambda_\theta \pi}{2 \cdot 1 \cdot 2\lambda_\theta} \cdot \frac{kT}{\pi} = \frac{kT}{2} .$$

It will also be convenient to have an expression for the mean kinetic energy of the galvanometer armature. Remembering that equation (3) relates to the potential energy of the galvanometer armature at any specific frequency, we may substitute for $U|\theta|^2$ its equal $K|\dot{\theta}|^2 \omega_g^2/\omega^2$. The equation corresponding to equation (5) may be written

$$\frac{K|\dot{\theta}|^2}{2}\Bigg|_1^2 = \int_1^2 \frac{2\lambda_\theta x^2}{(1 - x^2)^2 + 4\lambda_\theta^2 x^2} \cdot \frac{kT}{\pi}\, dx \qquad (6)$$

Similarily, the value of this integral also must be kT/2 over the range $\omega = o$ to $\omega = \infty$.

Again the denominator is expanded and factored to yield a standard integral form, which gives as a result

$$\int_o^\infty \frac{x^2\,dx}{(a^2 + x^2)(b^2 + x^2)} = \frac{\pi}{2(a + b)}$$

so that equation 6 integrates to

$$\frac{K|\dot{\theta}|^2}{2}\Bigg|_o^\infty = \frac{2\lambda_\theta\,\pi}{2 \cdot 2\lambda_\theta}\,\frac{kT}{\pi} = \frac{kT}{2}$$

It is instructive to consider the potential and kinetic energy in the galvanometer armature as functions of equal increments in frequency ratio rather than frequency difference. Rewriting equations (5) and (6) in the forms

$$\frac{U|\theta|^2}{2}\Bigg|_1^2 = \int_1^2 \frac{2\lambda_\theta\,\omega/\omega_g}{(1 - \omega^2/\omega_g^2)^2 + 4\lambda_\theta^2\,\omega^2/\omega_g^2} \cdot \frac{kT}{\pi}\,d(\ln \omega) \qquad (7)$$

and

$$\frac{K|\dot{\theta}|^2}{2}\Bigg|_1^2 = \int_1^2 \frac{2\lambda_\theta\,\omega^3/\omega_g^3}{(1 - \omega^2/\omega_g^2)^2 + 4\lambda_\theta^2\,\omega^2/\omega_g^2} \cdot \frac{kT}{\pi}\,d(\ln \omega) \qquad (8)$$

Similarily, the value of this integral also must be kT/2 over the range $\omega = o$ to $\omega = \infty$.

Again the denominator is expanded and factored to yield a standard integral form, which gives as a result

$$\int_o^\infty \frac{x^2\,dx}{(a^2 + x^2)(b^2 + x^2)} = \frac{\pi}{2(a + b)}$$

so that equation 6 integrates to

$$\frac{K|\dot{\theta}|^2}{2}\Bigg|_o^\infty = \frac{2\lambda_\theta\,\pi}{2 \cdot 2\lambda\theta} \quad \frac{kT}{\pi} = \frac{kT}{2}$$

It is instructive to consider the potential and kinetic energy in the galvanometer armature as functions of equal increments in frequency ratio rather than frequency difference. Rewriting equations(5)and(6)in the forms

$$\frac{U|\theta|^2}{2}\Bigg|_1^2 = \int_1^2 \frac{2\lambda_\theta\,\omega/\omega_g}{(1 - \omega^2/\omega_g^2)^2 + 4\lambda_\theta^2\,\omega^2/\omega_g^2} \cdot \frac{kT}{\pi}\,d(\ln\omega) \qquad (7)$$

and

$$\frac{K|\dot{\theta}|^2}{2}\Bigg|_1^2 = \int_1^2 \frac{2\lambda_\theta\,\omega^3/\omega_g^3}{(1 - \omega^2/\omega_g^2)^2 + 4\lambda_\theta^2\,\omega^2/\omega_g^2} \cdot \frac{kT}{\pi}\,d(\ln\omega) \qquad (8)$$

arranges the integrands so that their numerical values are proportional to the power out of a high Q, constant Q, filter centered on various frequencies in turn. Equation(7) would be used if the filter input voltage is proportional to galvanometer deflection about its mean position, while equation(8) is appropriate to a filter input proportional to the armature velocity with respect to its case.

The numerical value of an integrand at some particular frequency is the energy content (potential or kinetic) at that frequency per unit bandwidth. The unit bandwidth considered in equations(7) and(8) is that band whose edge frequencies are in the ratio e, the base of the natural logarithm. If the numerical value is multiplied by ln 2 = 0.693, it becomes the energy per octave.

In figure 2, the numerical values of these integrands have been plotted as ordinate with log (ω/ω_g) as abscissa for several values of λ_θ. The rectangle has an area of kT/2, and is the total area under any single curve.

The reader will note that while the above equations have been developed for a D'arsonval galvanometer they are equally valid for an open-circuit seismometer, whether of the moving-coil or variable-reluctance type.

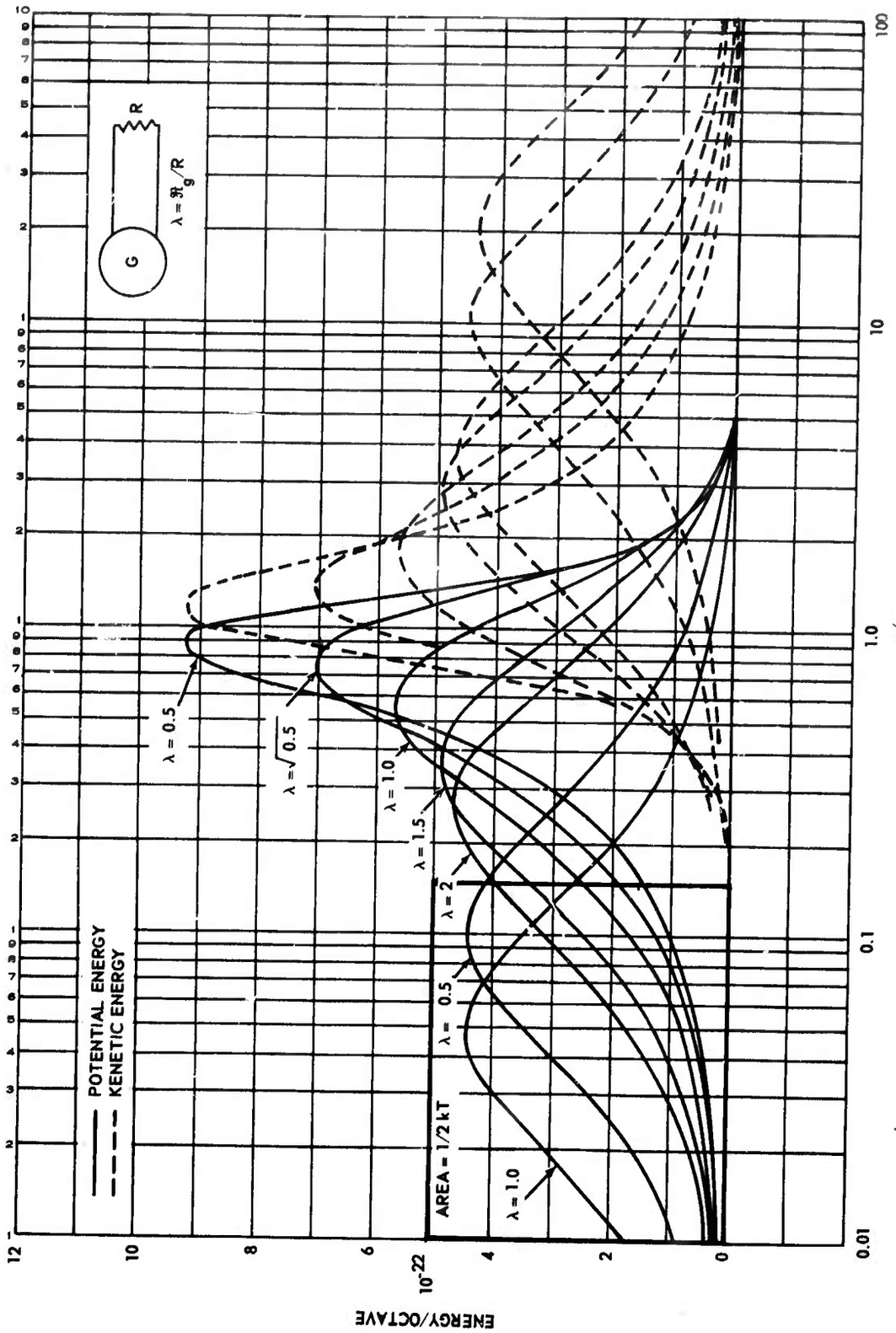

G 2379

Figure 2. Damped galvanometer

Since the impedance of a galvanometer depends upon frequency, the effect of an ideal (i.e. noise free), external resistor connected to a galvanometer might be expected to represent more than an attenuation, by a constant factor, of the energy in the galvanometer due to internal losses.

The equivalent electrical circuit is shown in figure 3, wherein the coil resistance has been lumped with the external resistance, as the resistor R, presumed ideal for the moment.

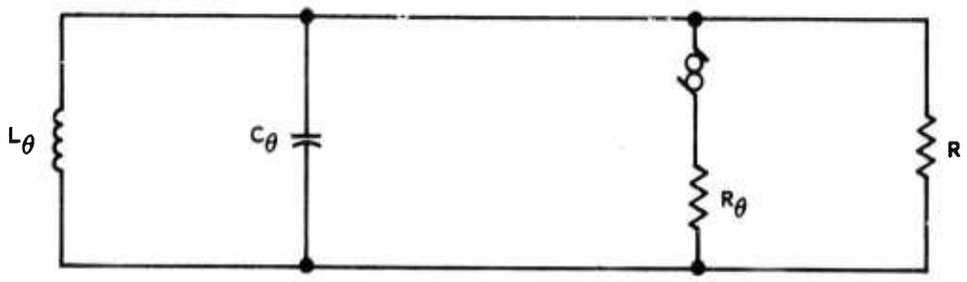

Figure 3. Equivalent electrical circuit of a galvanometer

Using the appropriate subscripts to designate the currents in the various branches, we may write

$$E_\theta = (i_\ell + i_c + i_R)\, R_\theta + i_\ell\, j\, \omega L_\theta \qquad (9)$$

Since $i_R\, R = i_\ell\, j\, \omega L_\theta$, this may be written

$$E_\theta = (i_\ell + i_c)\, R_\theta + i_\ell\, j\, \omega L_\theta + \frac{R_\theta}{R}\, i_\ell\, j\, \omega L_\theta$$

Remembering that $R_g/R = \lambda_g$, and performing the same algebraic manipulations and substitutions as before, one obtains

$$\frac{U|\theta|^2}{2}\Bigg|_1^2 = \int_1^2 \frac{2\,\lambda_\theta\, \omega/\omega_g}{(1 - \omega^2/\omega_g^2)^2 + 4\,(\lambda_\theta + \lambda_g)^2\, \omega^2/\omega_g^2} \cdot \frac{kT}{\pi}\, d\,(\ln \omega) \qquad (10)$$

It will be noted that this integrand is less than that of equation 7 at all real values of ω and the ratio of the two integrands is frequency dependent.

Since this integrand is less than that of equation 7 at all positive values of ω it follows that integrating equation 10 from $\omega = o$ to $\omega = \infty$ will give less than kT/2. That is, the presence of the external resistor modifies the transfer of energy from the internal damping resistance to the armature. There is no violation of the laws of thermodynamics as the presence of the external resistor modifies the transfer of energy from the armature to the internal damping resistor in precisely the same proportion.

From the symmetry of the resistors in figure 3, the equation for the hypothetical case of a noisy external resistor and an ideal internal damping can be written directly as

$$\frac{U|\theta|^2}{2}\Bigg|_1^2 = \int_1^2 \frac{2\lambda_g \omega/\omega_g}{(1-\omega^2/\omega_g^2)^2 + 4(\lambda_\theta + \lambda_g)^2 \omega^2/\omega_g^2} \cdot \frac{kT}{\pi} d(\ln \omega) \qquad (11)$$

In any real case both resistors will be noisy and since they are incoherent, their contributions to the energy of the galvanometer armature add directly. It is intuitively satisfying that several resistors in parallel, each considered as a separate noise source, give the same numerical result as a single equivalent noisy resistor.

In section 6.3 of NBS Report 7454, a number of potentially useful amplitude-frequency response curves were developed for a seismometer without

inductance directly coupled to a galvanometer. The internal losses of the two instruments were considered negligible so that the electrical analog in figure 4 is appropriate.

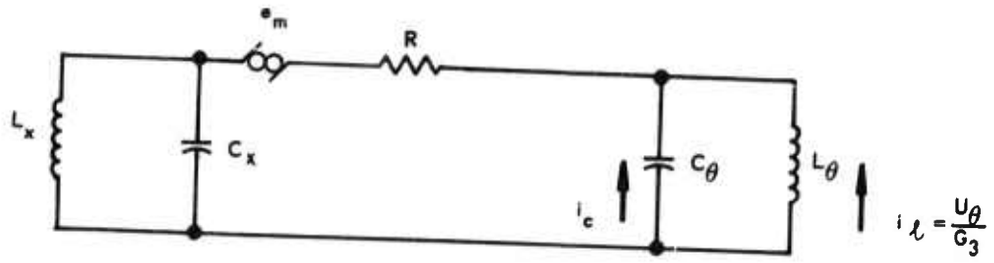

Figure 4. Seismometer-galvanometer combination

Here R includes the resistance of the two instrument coils and e_m is the thermal noise generator.

One would expect the presence of the seismometer to introduce a spectral region, centered on ω_o, in which the noise generator e_m would feed little or no energy into the galvanometer armature. That is, the seismometer should act as a notch filter of the energy transferred between the noisy resistor and the galvanometer armature.

Since the impedance of the seismometer can be written as $2\,j\,R_o\,\omega/\omega_o(1-\omega^2/\omega_o^2)$ the desired integral may be obtained from

$$e_m = (i_c + i_\ell)\left(R + 2\,j\,\frac{R_o\,\omega/\omega_o}{1-\omega^2/\omega_o^2}\right) + j\,\omega L_\theta\, i_\ell \qquad (12)$$

where $\omega_o^2 = 1/L_x C_x$ and $R_o = \omega_o L_x/2$.

Using the algebraic manipulations and substitutions indicated above, plus $\lambda_o = R_o/R$, the integral may be written

$$\frac{U|\theta|^2}{2}\Big|_1^2 = \int_1^2 \frac{2\lambda_g\,\omega/\omega_g}{\left(1-\frac{\omega^2}{\omega_g^2}\right) + 4\lambda_g^2\,\frac{\omega^2}{\omega_g^2}\left[\frac{(1-\omega^2/\omega_g^2)\,\lambda_o\,\omega_o}{\left(\frac{\omega_o^2}{\omega_g^2}-\frac{\omega^2}{\omega_g^2}\right)\lambda_g\,\omega_g}+1\right]^2}\cdot\frac{kT}{\pi}\,d(\ln\omega) \quad (13)$$

This equation can be integrated over the range ω=o to ω=∞, at least in principle.

Comparing the integrand of this equation with that of equation (7), several conclusions can be drawn by inspection.

(a) As $\lambda_o \rightarrow$ o, the two equations become identical. This is not surprising as it represents decoupling of the mechanical portions of the seismometer from the electrical circuit.

(b) At $\omega = \omega_o$, $\lambda_o \neq$ o, and $\omega_o \neq \omega_g$, the quantity within the bracket becomes infinite and the integrand becomes zero. The equation therefore shows anticipated notch filter effect due to the seismometer.

(c) With $\lambda_o \neq$ o for all values of ω outside the range from ω_o to ω_g, the numerical value of the bracket is greater than 1 so that the integrand is less than that of equation (7).

(d) With $\lambda_o \neq$ o and $\omega_o \neq \omega_g$, then for all values of ω lying between ω_o and ω_g, the quantity within the bracket is less than 1 and the value of the integrand is greater than that of equation (7).

(e) For the special case of $\lambda_o = \lambda_g$ and $\omega_o = \omega_g$, then at $\omega = \omega_o = \omega_g$ the value of this integrand is 1/4 the integrand of equation (7).

Shown in figure 5 is the value of the integrand of equation (13) for a four octave separation of instrument natural frequencies. As the equation is

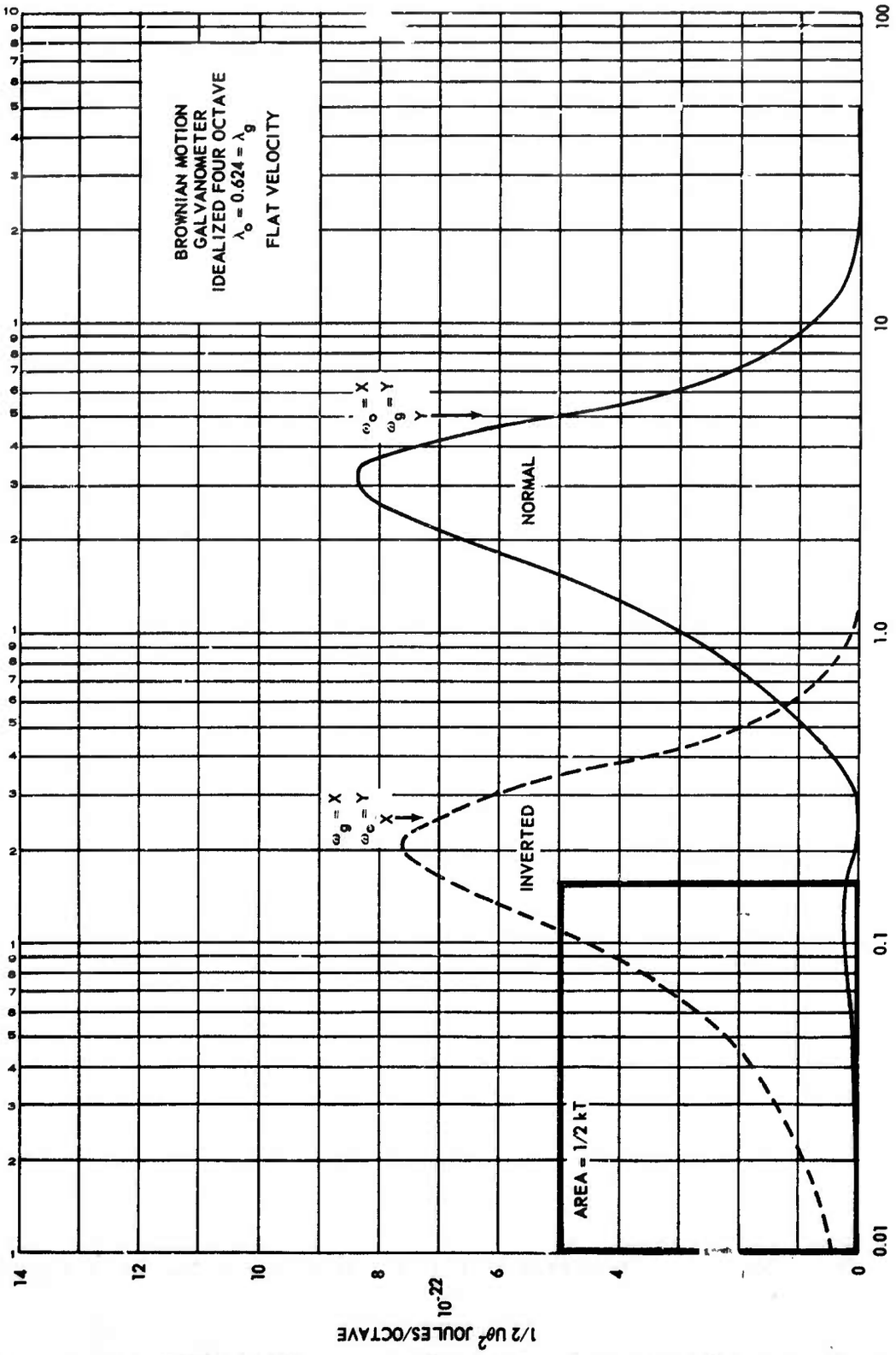

G 2381

Figure 5. Seismometer-galvanometer combination

not symmetrical with regard to an interchange of ω_o and ω_g, both $\omega_o < \omega_g$ and $\omega_g < \omega_o$ have been plotted. Selected are cases of constant velocity fourth order responses for which $\lambda_o = \lambda_g = 0.624$.

In developing the amplitude frequency response curves of seismometer galvanometer systems, the errors introduced by neglecting the internal losses of the instruments are small provided that the fraction of critical damping represented by these losses are small compared to that of the electrical circuit. In modern instrument design this is frequently the case.

On elementary grounds one can see that the effects of internal losses on the frequency distribution of Brownian motion may not be negligible. For instance, the presence of internal losses in the galvanometer will decrease the contribution of the series loop resistance at all frequencies, especially at ω_o. At the same time, the contribution of the galvanometer internal losses to the energy of the armature will be decreased by the presence of the series loop resistance except for $\omega \sim \omega_o$. The internal losses in the seismometer will contribute energy to the galvanometer armature at all frequencies and especially for $\omega \sim \omega_o$. Also, internal losses in the seismometer increase the contribution of the series loop resistance for $\omega \sim \omega_o$.

To develop the equations giving the separate contributions of the three noisy resistors to the galvanometer potential energy, the electrical analog in figure 6 will be used.

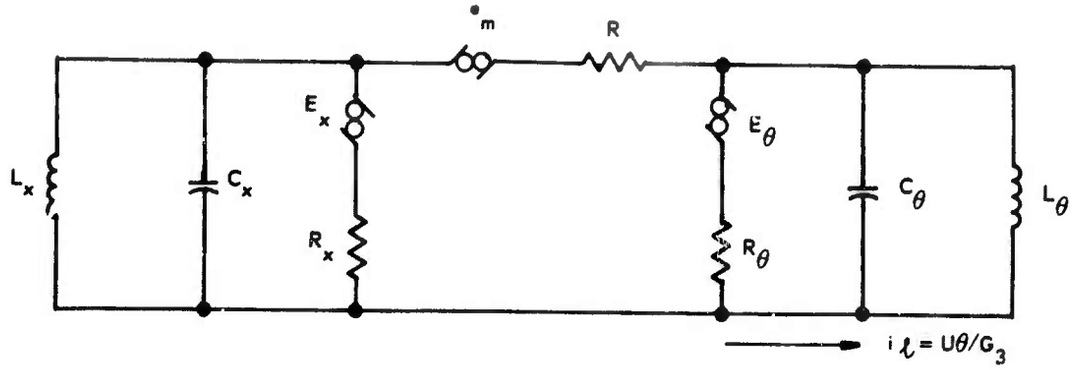

Figure 6. Seismometer-galvanometer combination with internal losses

For the contribution of E_θ to the galvanometer potential energy, one can obtain

$$\frac{U|\theta_e|^2}{2}\Big|_1^2 = \int_1^2 \frac{2\,\lambda_\theta}{D_r^2 + D_i^2}\left[4\,\Lambda_o^2 x^2 + \frac{\omega_g^2}{\omega_o^2}\left(\frac{\omega_o^2}{\omega_g^2} - x^2\right)^2\right]\frac{kT}{\pi}\,dx \qquad (14)$$

where

$$D_r = (1 - x^2)\left(\frac{\omega_o^2}{\omega_g^2} - x^2\right)\frac{\omega_g}{\omega_o} - 4\,x^2\,(\Lambda_o\,\Lambda_g - \lambda_o\,\lambda_g)$$

$$D_i = 2\,\Lambda_g\,x\left(\frac{\omega_o^2}{\omega_g^2} - x^2\right)\frac{\omega_g}{\omega_o} + 2\,\Lambda_o\,x\,(1 - x^2)$$

$$\Lambda_o = \lambda_o + \lambda_x$$

$$\Lambda_g = \lambda_g + \lambda_\theta$$

as the contribution of galvanometer internal losses to the potential energy of the galvanometer armature.

The effect of e_m on the galvanometer armature results in

$$\left.\frac{U|\theta_m|^2}{2}\right|_1^2 = \int_1^2 \frac{2\lambda_g}{D_r^2 + D_i^2} \left[4\lambda_x^2 x^2 + \frac{\omega_g^2}{\omega_o^2}\left(\frac{\omega_o^2}{\omega_g^2} - x^2\right)^2\right] \frac{kT}{\pi}\, dx \qquad (15)$$

The third integral of interest is that relating the contribution of F_x to the energy of the galvanometer, which results in

$$\left.\frac{U|\theta_x|^2}{2}\right|_1^2 = \int_1^2 \frac{2\lambda_x}{D_r^2 + D_i^2} \left[4\lambda_o \lambda_g x^2\right] \frac{kT}{\pi}\, dx \qquad (16)$$

Combining these three equations one can obtain

$$\left.\frac{U|\theta|^2}{2}\right|_1^2 = \int_1^2 \frac{2\Lambda_g}{D_r^2 + D_i^2} \left[4\Lambda_o^2 (1 - \alpha^2) x^2 + \frac{\omega_g^2}{\omega_o^2}\left(\frac{\omega_o^2}{\omega_g^2} - x^2\right)^2\right] \frac{kT}{\pi}\, dx \qquad (17)$$

where

$$\alpha^2 = \lambda_g \lambda_o / \Lambda_g \Lambda_o$$

as the effect of the system's thermal noise level on the potential energy of the galvanometer armature.

It is of interest to note that α is the geometric mean of the fraction of the total damping which is internal to the two instruments.